Technical Report Documentation Page

1. Report No.	2. Government Accession No.	3. Recipient's Catalog No.

4. Title and Subtitle

ANTHROPOMETRIC SPECIFICATIONS FOR MID-SIZED MALE DUMMY, Volume 2

5. Report Date
December 1983

6. Performing Organization Code

7. Author(s)
D.H. Robbins

8. Performing Organization Report No.
UMTRI-83-53-2

9. Performing Organization Name and Address
The University of Michigan
Transportation Research Institute
2901 Baxter Road
Ann Arbor, Michigan 48109

10. Work Unit No. (TRAIS)

11. Contract or Grant No.
DTNH22-80-C-07502

12. Sponsoring Agency Name and Address
U.S. Department of Transportation
National Highway Traffic Safety Administration
Washington, D.C. 20590

13. Type of Report and Period Covered
FINAL REPORT
Oct. 1980 - Dec. 1983

14. Sponsoring Agency Code

15. Supplementary Notes

Vol. 1: Development of Anthropometrically Based Design Specifications for an Advanced Adult Anthropomorphic Dummy Family
Vol. 3: Anthropometric Specifications for Small Female & Large Male Dummies

16. Abstract

The purpose of this report is to present the anthropometric specifications for a mid-sized male dummy. Data gathered during the project as well as data available in the literature were used in formulating these specifications. The analytical techniques and procedures used in combining the various data resources are described.

This report is part of a package which also includes schematic drawings and a reference standard surface form. The schematic drawings show front, side, and top views of the dummy form with key landmarks and segmentation dimensioned with respect to the standard seat coordinate system. These three drawings are supplemented by front and side full-size drawings with a superimposed skeletal rendering. The full-size seated surface form is based on a clay model.

17. Key Words	18. Distribution Statement
Anthropometry Crash Test Dummy	Unlimited

19. Security Classif. (of this report)	20. Security Classif. (of this page)	21. No. of Pages	22. Price
None	None	134	

This document is disseminated under the sponsorship of the Department of Transportation in the interest of information exchange. The United States Government assumes no liability for the contents or the use thereof.

NOTICE

The rights, welfare, and informed consent of the volunteer subjects who participated in this study were observed under guidelines established by the U.S. Department of Health, Education and Welfare Policy (now Health and Human Services) on Protection of Human Subjects and accomplished under medical research design protocol standards approved by the Committee to Review Grants for Clinical Research and Investigation Involving Human Beings, Medical School, The University of Michigan.

VOLUME 2: CONTENTS

LIST OF TABLES

LIST OF FIGURES

1.0 INTRODUCTION

The purpose of Volume 2 is to present the anthropometric specifications for a mid-sized male dummy. Data gathered during the project as well as data available in the literature were used in formulating these specifications. This volume is organized not only to present the results, but to lead the user through the process of development of a consistent anthropometric description of a seated human.

The first sections concentrate on subject geometric definition based on measured surface landmarks and the construction of a standard seat coordinate system in which all data can be specified. In the next sections, the emphasis shifts to division of the body into discrete segments. This implies at least partial acceptance of the assumption that the human body can be represented as a chain of rigid bodies in dynamic applications. (In the static sense, when the body is not moving, this assumption is valid.) Individual coordinate systems are defined for each segment. Transformations are developed which relate these segment systems to the standard seat coordinate system. Mathematical formulations follow for the construction of segmentation planes between the various parts of the body. The static anthropometric description is completed by estimation of joint center locations for the seated subject in both standard seat and segment coordinate systems.

A step toward dynamic anthropometric specifications is made in the concluding sections of the report. The limited consistent information available for description of mobility between the various segments of the body is reviewed. The results are assembled into a qualified specification on range of motion to complete the report.

This report is supplemented by full-size blueprints (Nos. MM-101, MM-102, MM-103, MM-104, MM-105) showing side, front, and top views of the following:

- Surface landmarks
- Joints centers
- Segment centers of gravity

- Origins of segment coordinate systems
- Surface profile of actual surface form
- Information on anatomical and principal axes
- Information on segmentation planes
- A superimposed skeletal rendering

Figure 1 in this report is a schematic showing a subset of this information.

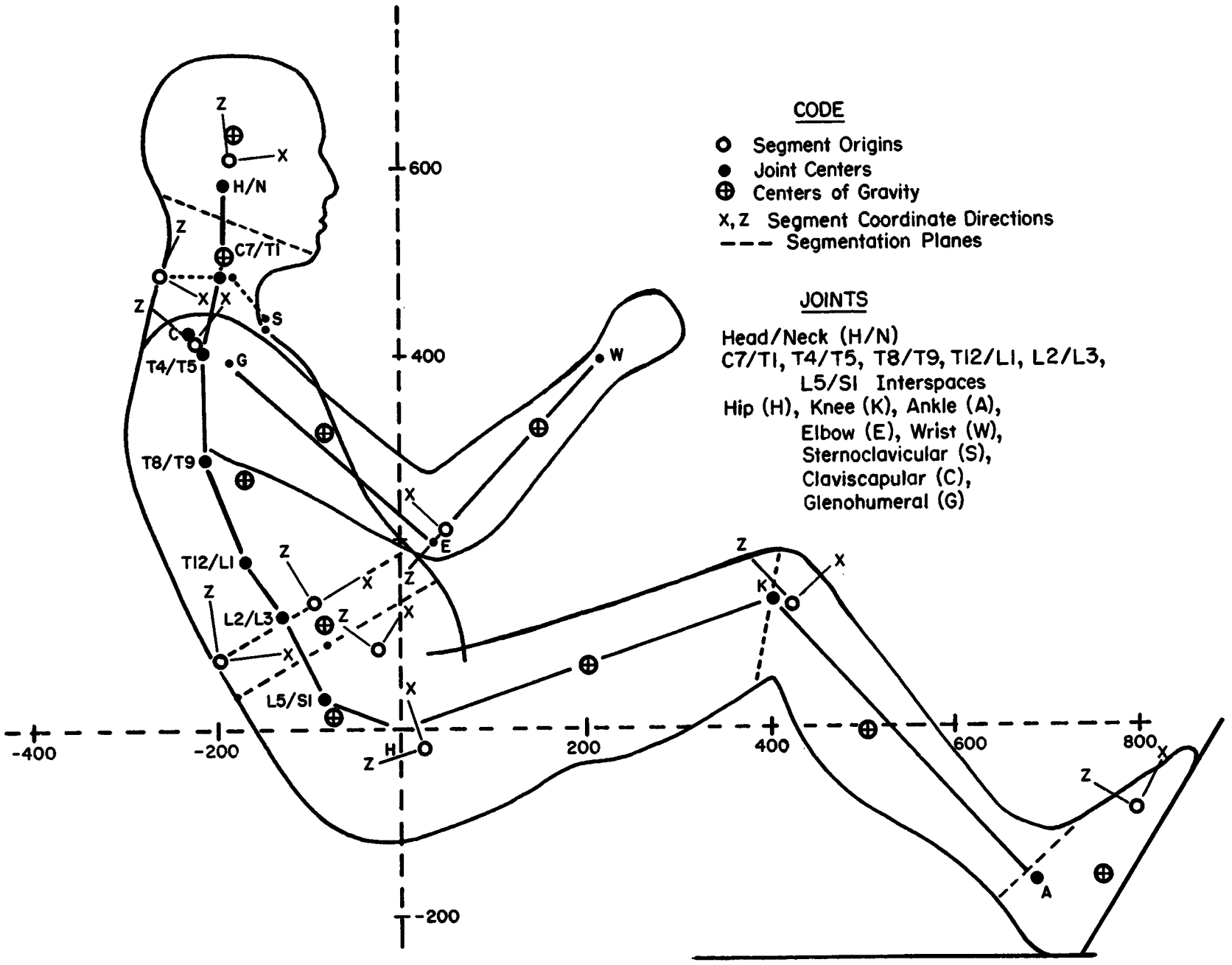

FIGURE 1. Anthropometric specifications for mid-sized male dummy.

2.0 LANDMARKS USED FOR SUBJECT DEFINITION

In order to develop a geometric and mass definition of a person seated in an automobile it is necessary to take into account a variety of issues including:

- Body segmentation scheme
- Sizing of components
- Segment masses
- Segment centers of gravity
- Segment moments of inertia
- Joint locations
- Joint ranges of motion
- Surface geometry
- Orientation of pelvis, vertebral column, skull, and lower extremities in the seated position
- Relation of coordinate systems in anatomical segments to the standard seat coordinate system

Table 1 is the original minimum collection of geometric points estimated to be required. The first thirty-one are minimum requirements for body segmentation, mass property definition, and segment coordinate system construction using the formulae and techniques of McConville et al. (1980). Tables 2 and 3 associate particular skeletal landmarks used in the present analysis with coordinate systems and segmentation planes. The large majority of these agree with the first thirty-one of Table 1. However, a few new points can be identified which are required for the study of seated posture. These include points to define the:

- Thorax and abdomen coordinate system and the thorax segmentation plane: "Intersection point on the back of the surface form of a perpendicular from the center of a line connecting the 10th rib targets to a line connecting the T12 and L5 surface targets."

- Foot coordinate system: "Heel point" (taken directly from the seating buck).

- Abdomen segmentation plane: "Intersection point on the back of the surface form of a perpendicular from the center of a line connecting the iliocristale targets to a line connecting the L2 and L5 surface targets."

- Hip segmentation plane: "Pubotuberosity" and "lateral tuberosity point."

Beyond the first thirty-one, the next three landmarks locate the position of the scapula within the space defined by a shoulder girdle mass, which is separate from the thorax or chest mass defined by McConville et al. Although it has not been possible within the current activity, it is recommended that in future work the cadaver shoulder girdle segmentation scheme and mass data of Dempster (1965) be used to decompose the thorax definition of McConville into rib cage and shoulder girdle segments. The recognition of the separation of rib cage from shoulder girdle will lay the basis for design of more realistic interactions between members of the new dummy family and side door structures as well as frontal restraint devices. A further purpose is to more clearly define the location of the acromio-clavicular and glenohumeral joints so that the best possible estimates of shoulder girdle centers of rotation can be made.

The final five surface landmarks relate to the spinal column. These data are being used as input for procedures reported by Snyder et al. (1972) to define the location of several spinal interface centers with respect to the surface data. These landmarks are important for placing the vertebral column in a correct relationship to the exterior of the surface form.

Four of the surface landmarks in Table 1 require special comment. These are marked by asterisks. The symphysion was replaced in the final list of subject targets by pelvic crest due to the difficulty of target location for photographic data acquisition. In order to compensate, a correction factor was developed to translate pelvic crest landmark to symphysion based on pelvic geometry data of Reynolds et al. (1981). Posterior calcaneus is hidden from view in that the heel is in the driving position in the standard seat buck. However, a close approximation of this point is the heel point reference which is measured directly on the buck.

It was not possible to obtain two points directly. These are nuchale and gluteal furrow. However, nuchale position can be inferred from the surface form and by the fact that its location is given in anatomical coordinates by McConville et al. (1980). Gluteal furrow point is in contact with the seat and hence is invisible. No attempt to

develop this point was made because of tissue shifts between standing seated posture. The subject is discussed further in Sections 5 and 6.

TABLE 1

LIST OF SURFACE LANDMARKS FOR SEGMENT AND JOINT DEFINITION
(Original Requirements)

1. Cervicale*
2. Acromion
3. Trochanterion (skeletal reconstruction)
4. Infraorbitale
5. Tragion
6. Suprasternale
7. Lateral Humeral Epicondyle
8. Ulnar Styloid
9. Anterior-Superior Iliac Spine
10. Symphysion**
11. Lateral Femoral Epicondyle
12. Lateral Malleolus
13. Clavicale
14. Mid-Spine, 10th Rib Level
15. Lateral 10th Rib
16. Medial Humeral Epicondyle
17. Radiale
18. Stylion
19. Medial Femoral Epicondyle
20. Tibiale
21. Sphyrion
22. Metatarsal/Phalangeal I
23. Metatarsal/Phalangeal V
24. Posterior Calcaneus**
25. Tip of Digit II (Toe)
26. Gonion
27. Iliocristale
28. Anterior Scye
29. Olecranon
30. Nuchale**
31. Gluteal Furrow (most inferior point)**
32. Superior Margin Scapula
33. Inferior Margin Scapula
34. Acromio-Clavicular Articulation
35. T4 Surface
36. T8 Surface
37. T12 Surface
38. L2 Surface
39. L5 Surface

*See Section 3.0 in Volume 1 for definitions.

**Landmarks modified or deleted from final list.

TABLE 2

LANDMARKS USED IN CONSTRUCTION OF SEGMENT ANATOMICAL COORDINATE SYSTEMS

Segment	Landmarks
Head	Tragion (L and R) Infraorbitale (L)
Neck	Clavicale (L and R) Cervicale
Thorax	Cervicale 10th rib (L and R) Intersection point on back of surface form of a perpendicular from the center of a line connecting the 10th rib targets to a line connecting the T12 and L5 surface targets T12 L5
Abdomen	10th rib (L and R) Intersection point on back of surface form of a perpendicular from the center of a line connecting the 10th rib targets to a line connecting the T12 and L5 surface targets T12 L5
Pelvis	Anterior-Superior Iliac Spines (L and R) Symphysion
Upper Arms	Acromion (L and R) Medial Humeral Epicondyle (L and R) Lateral Humeral Epicondyle (L and R)
Lower Arms and Hands	Radiale (L and R) Ulnar Styloid Process, Distal End (L and R) Radial Styloid Process, Distal End (L and R)
Upper Legs	Trochanterion, reconstructed (L and R) Lateral Femoral Epicondyle (L and R) Medial Femoral Epicondyle (L and R)
Lower Legs	Tibiale (L and R) Sphyrion (L and R) Lateral Malleolus (L and R)
Feet	Metatarsal/Phalangeal I (L and R) Metatarsal/Phalangeal V (L and R) Heel Point (L and R)

TABLE 3

LANDMARKS USED IN CONSTRUCTING SEGMENTATION PLANES

Segmentation Plane	Landmarks
Head	Gonion (L and R) Nuchale
Neck	Clavicale Cervicale
Thorax	10th Rib (L and R) Intersection point on back of surface form of a perpendicular from the center of a line connecting the 10th rib targets to a line connecting the T12 and L5 surface targets
Abdomen	Iliocristale (L and R) Intersection point on back of surface form of a perpendicular from the center of a line connecting the iliocristale targets to a line connecting the T12 and L5 surface targets
Hip	Anterior-Superior Iliac Spine (L and R)* Pubotuberosity (L and R)* Lateral Tuberosity Point (L and R)*
Knee	Lateral Femoral Epicondyle (L and R)
Ankle	Sphyrion (L and R)
Shoulder	Acromion (L and R) Anterior Scye (L and R) Posterior Scye (L and R)
Elbow	Olecranon Medial Humeral Epicondyle Lateral Humeral Epicondyle

*These skeletal landmarks are derived from the position in space of the average pelvis (Reynolds et al. 1981).

3.0 DEVELOPMENT OF STANDARD SEAT COORDINATE SYSTEM

The selection of a standard seat coordinate system was made between two candidates: (1) traditional H-point, and (2) seat-based coordinate system. The traditional H-point represents a point on the H-point machine associated with the human hip joint. Seat-based coordinate systems often reflect the intersection point between seat back and seat cushion lines. The continuous curvature of the seat back and cushion of the average standard seat developed on this project prevented development of any clear definition of seat back and seat cushion lines. Hence, it was decided that the traditional H-point concept offered the better alternative.

The surface landmarks for right and left anterior-superior iliac spines as well as pelvic crest were obtained in this study (see Volume 1, Section 3.8). These were used to determine the orientation of the pelvis in three-dimensional coordinates. In order to define the H-point it was necessary to estimate tissue thicknesses of the surface landmarks over the skeletal landmarks. These data also being available, it was then possible to orient the pelvis if an appropriate average structure could be found.

The pelvic data of Reynolds et al. (1981) are based on a subject group similar in average stature and weight to those measured during the current UMTRI study as shown below.

Body Measurement	UMTRI 1983	Reynolds et al. 1981
Weight (lb)	168.8	165.7
Stature (cm)	175.1	173.6

These data were accepted for the pelvic reconstruction, location of the standard seat coordinate system at the center of a line connecting the H-points, location of the center of rotation of the two hip joints, and location of the lumbar-sacral (L5/S1) joint center.

The direction of Reynolds' coordinate system was superimposed upon the UMTRI data for anterior-superior iliac spine (ilio-spinale summum) and pubic symphysis (Figure 2). The direction of 54.07 degrees between the two allowed conversion of any of the Reynolds et al. data points into a system parallel to the UMTRI lab system with an origin at the center point of the anterior-superior iliac spines using the simple transformation:

$$X_L = X_R \cos\theta - Z_R \sin\theta$$

$$Z_L = X_R \sin\theta + Z_R \cos\theta$$

where the subscript R identifies the Reynolds et al. coordinate values and L refers to the lab system. The following points were transformed as needed for use in construction of joint centers, segmentation planes, anatomical segment axis construction, estimation of tissue depths, etc.:

- H-points
- Pubic symphysis
- Inferior symphyseal pole
- Superior pole, pubic symphysis
- Ilio-spinale summum
- Ilio-cristale summum
- Inferior tuberosity point
- Posterior point on 1st sacral vertebral body
- Promontorion
- Lateral point on 1st sacral vertebral body
- Pubotuberosity
- Lateral tuberosity point

The key points for development of a standard seat coordinate system were the H-points which have the following coordinates in the UMTRI laboratory reference system (defined by the subscript L):

H-Point	X_L (mm)	Y_L (mm)	Z_L (mm)
Left	657	701	422
Right	657	537	422

The Y-shift from the body centerline was ±82 mm as reported by Reynolds et al. The center of the line connecting these two points is located at: X_L=657, Y_L=619, Z_L=422. This point is selected as the origin of the standard seat coordinate system. All further data in this report are

related to this point on the body centerline. The subscript for all data quantities referred to in this new coordinate system based on the H-point will have the subscript H.

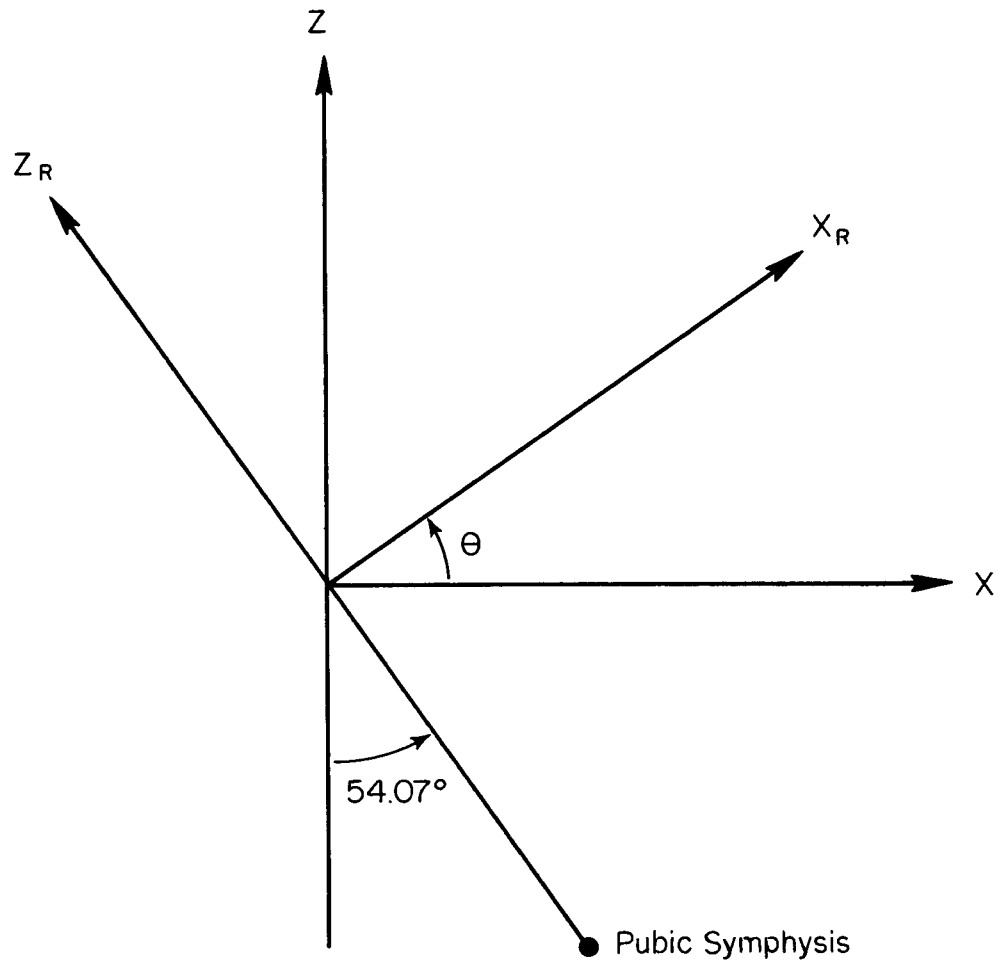

FIGURE 2. Pelvic coordinate system superimposed on UMTRI lab-based coordinate system.

4.0 SUBJECT DATA TRANSLATED TO STANDARD COORDINATE SYSTEM

Table 4 presents all skeletal and surface landmarks used in the development of the anthropometric specifications for the mid-sized male dummy and are incorporated in the surface form. The origin of coordinates is the center of a line connecting the H-points. These data are derived from the original data given in Volume 1 of this report. The subscript H is used throughout the report for all quantities given with respect to this origin.

TABLE 4

SKELETAL AND SURFACE LANDMARKS RELATIVE TO H-POINT (mm)

Body Segment and Landmark	Surface			Skeletal		
	X_H	Y_H	Z_H	X_H	Y_H	Z_H
HEAD						
Glabella	- 80	0	651	- 87	0	651
Infraorbitale (L)	- 96	34	620	- 99	34	620
Infraorbitale (R)	- 96	- 34	620	- 99	- 34	620
Tragion (L)	-185	83	614	-185	76	614
Tragion (R)	-185	- 83	614	-185	- 76	614
Gonion (L)	-173	70	544	-173	67	549
Gonion (R)	-173	- 70	544	-173	- 67	549
Gnathion	-101	0	511	-107	0	517
Nuchale*	-262	0	579			
VERTEBRAL COLUMN						
C7	-266	0	489	-258	0	489
T4	-293	0	380	-287	0	380
T8	-284	0	253	-274	0	253
T12	-246	0	146	-240	0	146
L2	-217	0	87	-212	0	87
L5	-174	0	13	-169	0	13
Mid-Spine 10th Rib	-242	0	138	-242	0	138
Superior Margin Scapula (L)	-296	79	403	-285	79	392
Superior Margin Scapula (R)	-296	- 79	403	-285	- 79	392
Inferior Margin Scapula (L)	-276	126	267	-269	126	274
Inferior Margin Scapula (R)	-276	-126	267	-269	-126	274
Intersection point on back of surface form of a perpendicular from center of line connecting 10th rib targets to line connecting T12 and L5 surface targets*	-209	0	71			
Intersection point on back of surface form of a perpendicular from center of line connecting iliocristale targets to line connecting T12 and L5 surface targets*	-188	0	35			
TORSO						
Suprasternale	-139	0	435	-140	0	431
Mesosternale	- 98	0	385	-101	0	385
Substernale	- 72	0	336	- 75	0	336
Bimammary, midline	- 52	0	281			
Nipple (L)	- 52	113	290			
Nipple (R)	- 52	-113	290			
10th Rib, Anterior, Midline	15	0	191			
Umbilicus	35	0	153			

TABLE 4
SKELETAL AND SURFACE LANDMARKS RELATIVE TO H-POINT (Continued)

Body Segment and Landmark	Surface			Skeletal		
	X_H	Y_H	Z_H	X_H	Y_H	Z_H
TORSO (Contd.)						
Maximum Abdominal Protrusion	56	0	129			
10th Rib (L)	- 93	156	133	- 93	136	133
10th Rib (R)	- 93	-156	133	- 93	-136	133
PELVIS						
Trochanterion (L) (UMTRI photo)	- 33	188	28	- 33	148	28
Trochanterion (R) (UMTRI photo)	- 33	-188	28	- 33	-148	28
Iliocristale (L)	- 80	161	93	- 80	131	93
Iliocristale (R)	- 80	-161	93	- 80	-131	93
Anterior-Superior Iliac Spine (L)	- 25	116	83	- 25	116	78
Anterior-Superior Iliac Spine (R)	- 25	-116	83	- 25	-116	78
Pubic Symphysis	51	0	41	44	0	28
Thigh/Abdominal Junction (L)	21	122	81			
Thigh/Abdominal Junction (R)	21	-122	81			
Trochanterion (skeletal reconstruction)*	20	±203	- 20			
H-Point				0	± 82	0
Pubic Symphysis				38	0	32
Inferior Symphyseal Pole				42	± 5	- 7
Left Superior Pole, Pubic Symphysis				33	4	25
Ilio-Spinale Summum				- 25	±115	78
Iliocristale Summum				-102	±119	74
Inferior Tuberosity Point				37	± 39	- 61
Posterior Point 1st Sacral Vertical Body				- 98	0	33
Promontorion				- 69	0	37
Lateral Point 1st Sacral Vertical Body				- 89	± 26	39
Pubotuberosity				34	± 25	29
Lateral Tuberosity				20	± 67	- 55
SHOULDER						
Clavicale (L)	-145	23	443	-147	23	439
Clavicale (R)	-145	- 23	443	-147	- 23	439
Acromio-Clavicular Articulation (L)	-215	182	443	-215	182	437
Acromio-Clavicular Articulation (R)	-215	-182	443	-215	-182	437
Greater Tubercle Humerus (L)	-173	218	421	-183	197	400
Greater Tubercle Humerus (R)	-173	-218	421	-183	-197	400
Acromion (L)	-224	203	419	-224	199	417
Acromion (R)	-224	-203	419	-224	-199	417
Anterior Scye (L)	- 97	154	380			
Anterior Scye (R)	- 97	-154	380			
Posterior Scye (L)	-214	197	306			
Posterior Scye (R)	-214	-197	306			

TABLE 4
SKELETAL AND SURFACE LANDMARKS RELATIVE TO H-POINT (Continued)

Body Segment and Landmark	Surface			Skeletal		
	X_H	Y_H	Z_H	X_H	Y_H	Z_H
ARM						
Lateral Humeral Epicondyle (L)	32	242	224	32	240	221
Lateral Humeral Epicondyle (R)	32	-242	224	32	-240	221
Radiale (L)	46	243	209	46	240	205
Radiale (R)	46	-243	209	46	-240	205
Medial Humeral Epicondyle (L)	32	173	199	32	176	202
Medial Humeral Epicondyle (R)	32	-173	199	32	-176	202
Olecranon (L)	53	210	186	53	210	189
Olecranon (R)	53	-210	186	53	-210	189
Ulnar Styloid (L)	226	191	387	226	191	388
Ulnar Styloid (R)	226	-191	387	226	-191	388
Stylion (L)	211	135	399	209	137	397
Stylion (R)	211	-135	399	209	-137	397
LEG AND FOOT						
Lateral Femoral Epicondyle (L)	404	189	129	404	185	129
Lateral Femoral Epicondyle (R)	404	-189	129	404	-185	129
Medial Femoral Epicondyle (L)	407	87	142	407	93	142
Medial Femoral Epicondyle (R)	407	- 87	142	407	- 93	142
Tibiale (L)	424	88	128	424	94	128
Tibiale (R)	424	- 88	128	424	- 94	128
Patella (L)	449	150	172			
Patella (R)	449	-150	172			
Sphyrion (L)	684	61	-149	684	63	-149
Sphyrion (R)	684	- 61	-149	684	- 63	-149
Metatarsal/Phalangeal I (L)	796	84	- 86	796	86	- 86
Metatarsal/Phalangeal I (R)	796	- 84	- 86	796	- 86	- 86
Digit II (L)	839	147	- 37	839	147	- 43
Digit II (R)	839	-147	- 37	839	-147	- 43
Metatarsal/Phalangeal V (L)	785	174	-124	785	173	-124
Metatarsal/Phalangeal V (R)	785	-174	-124	785	-173	-124
Lateral Malleolus (L)	680	126	-185	680	124	-181
Lateral Malleolus (R)	680	-126	-185	680	-124	-181

*Landmark location determined by construction.

5.0 SEGMENTATION AND LINKAGE SELECTION

The traditional segmentation of the human body for use in developing crash test device linkages is as follows:

Head	Two Lower Legs
Neck	Two Feet
Thorax	Two Upper Arms
Abdomen	Two Lower Arms
Pelvis	Two Hands
Two Upper Legs	

Although substantial mobility in the shoulder girdle has been known for years (see Dempster 1965, Dempster and Gaughran 1967, and Snyder et al. 1972), only minimal data are available for the description of its mass and inertial properties. Dempster (1965) reports a center of gravity, mass, and inertial properties around the side-to-side axis (Y-axis) for the masses associated with scapula, clavicle, and soft tissues exterior to most of the bony thorax. No shoulder girdle data are given in the more recent work of McConville et al. (1980) and Reynolds et al. (1975). As a result, it was concluded that insufficient consistent data are available from the literature to construct a separate shoulder girdle within the scope of the current activity.

A non-traditional segmentation scheme is recommended for the eventual advanced dummy family that includes a separate, mobile shoulder girdle link and the associated mass. Sufficient surface landmarks are available in the UMTRI data (scapula, clavicale, extent of rib cage) to define this segmentation. Mass, center of gravity, and inertial properties could be measured directly from a solid casting of the surface form shoulder girdle after separation from the thorax. Also, it is expected that a related mathematical procedure could be used to separate thorax from shoulder in the McConville et al. (1980) data.

In conclusion, the traditional segmentation and linkage system has been adopted as the only one feasible based on available data. It has been simplified slightly by coupling hand and lower arm masses, although the location of the wrist joint is specified. This linkage arrangement will be assumed throughout the remainder of the report.

6.0 CONSTRUCTION OF SEGMENTATION PLANES

The construction of segmentation planes is based largely upon the scheme used by McConville et al. (1980) in their determination of anthropometric relationships of body and body segment moments of inertia. The constructions are modified somewhat to account for differences between body segment relationships in the seated and standing postures.

6.1 Head Plane

The head plane is defined to pass through the left and right gonial points and the nuchale for a standing subject. As head orientation is very similar for both standing and seated posture, it is assumed that the procedure can be directly adopted. The gonial points are available from UMTRI measurements. However, the nuchale was estimated from values given in the McConville et al. report. To accomplish this, nuchale coordinates in the head anatomical coordinate system were rotated and translated into the UMTRI standard seat coordinate system. The three points defining the head segmentation plane are therefore:

Point	X_H (mm)	Y_H (mm)	Z_H (mm)
Nuchale	-279	0	579
Gonion (L)	-173	70	544
Gonion (R)	-173	- 70	544

The formula for this plane is:

$$.31354X_H + .94958Z_H - 462.33 = 0$$

It should be noted that formulae for segmentation planes can be used to determine the intersection of the plane with the surface form at points other than surface landmarks used in the definitions.

6.2 Neck Plane

The neck segmentation consists of two planes. The first plane is parallel to the floor and anterior to cervicale. The second plane originates at the clavicale and tilts up and back at a 45-degree angle until it intersects with the horizontal plane. Because the orientation of head and neck are similar in the seated and standing postures, this procedure was adopted directly from McConville et al. The points used for the construction were:

Point	X_H (mm)	Y_H (mm)	Z_H (mm)
Cervicale	-266	0	489
Clavicale	-145	± 23	443

The two planes were found to intersect along the line defined by X_H=191, Z_H=489. The formula for the first plane anterior to the cervicale is:

$$Z_H = 489 \qquad \text{for } X_H \leq -191.$$

The formula for the second plane is:

$$.70710X_H + .70710Z_H - 210.72 = 0 \qquad \text{for } X_H \geq -191.$$

6.3 Thorax Plane

The McConville et al. definition specifies that the plane originates at the 10th rib mid-spine landmark and passes through the torso parallel with the standing surface. In order to approximate this plane in the seated posture, a line was constructed from the 10th rib landmark which was perpendicular to a line connecting the T12 and L5 surface landmarks. This line, which is roughly perpendicular to the body centerline, is intended to separate the thorax which has a bony skeletal periphery from the abdomen which has a soft tissue periphery. In dynamic applications, thorax and abdomen will have very different stiffnesses and are coupled very differently to the bony skeleton. The points used in construction of the plane are:

Point	X_H (mm)	Y_H (mm)	Z_H (mm)
R10/Back Perpendicular	-209	0	71
R10	- 93	±156	133

The formula for the thorax plane is:

$$.47138X_H - .88194Z_H + 161.14 = 0$$

It should be noted that the L2 surface landmark is approximately 17 mm from the plane and the L2/L3 joint center falls less than 10 mm above the plane (see Figure 3).

6.4 Abdomen Plane

The McConville et al. definition specifies that the plane "originates at the iliocristale landmarks and passes through the torso parallel with the standing surface." This plane presents a dilemma even more complex than the thorax. Because of the spinal tilt due to the seated posture, it would seem logical to develop a segmentation scheme similar to that used for the thorax.

However, on the basis of the physical nature of the abdomen mentioned in Section 6.3, it would make more sense to define a scheme which better delineates the extent of the soft abdomen. A pair of new planes can be proposed, the first of which angles backward from the iliocristale landmarks perpendicular to the same line connecting the T12 and L5 surface landmarks which was used in constructing the thorax plane (see Figure 3). The second plane is horizontal and extends from the iliocristale target to the front of the body. The region of maximum abdominal protrusion is included in this definition. This planes passes just above the anterior-superior iliac spine targets and about 50 mm above pubic symphysis.

Two more observations on the McConville et al. data conclude the information required for making a final decision on the abdomen segmentation plane. The first is that the distance between the thorax and abdomen planes, which are parallel, is similar to the distance from the iliocristale landmark to the thorax segmentation plane developed from the UMTRI data. The second is that the data which are available for mass and inertial properties apply only to the parallel planes through the iliocristale and 10th rib landmarks.

CODE

JOINTS (T12/L1, L2/L3, L5/S1, HIP)
T12 - T12 LANDMARK
L2 - L2 LANDMARK
R10⊥ - POINT ON SURFACE FROM R10
I⊥ - POINT ON SURFACE FROM ILIOCRISTALE
L5 - L5 LANDMARK
R10 - 10th RIB LANDMARK
I - ILIOCRISTALE LANDMARK
U - UMBILICUS LANDMARK
M - MAXIMUM ABDOMINAL PROTRUSION
ASIS - ANTERIOR SUPERIOR ILIAC SPINE
TH - THORAX SEGMENTATION PLANE
AB - ABDOMEN SEGMENTATION PLANE

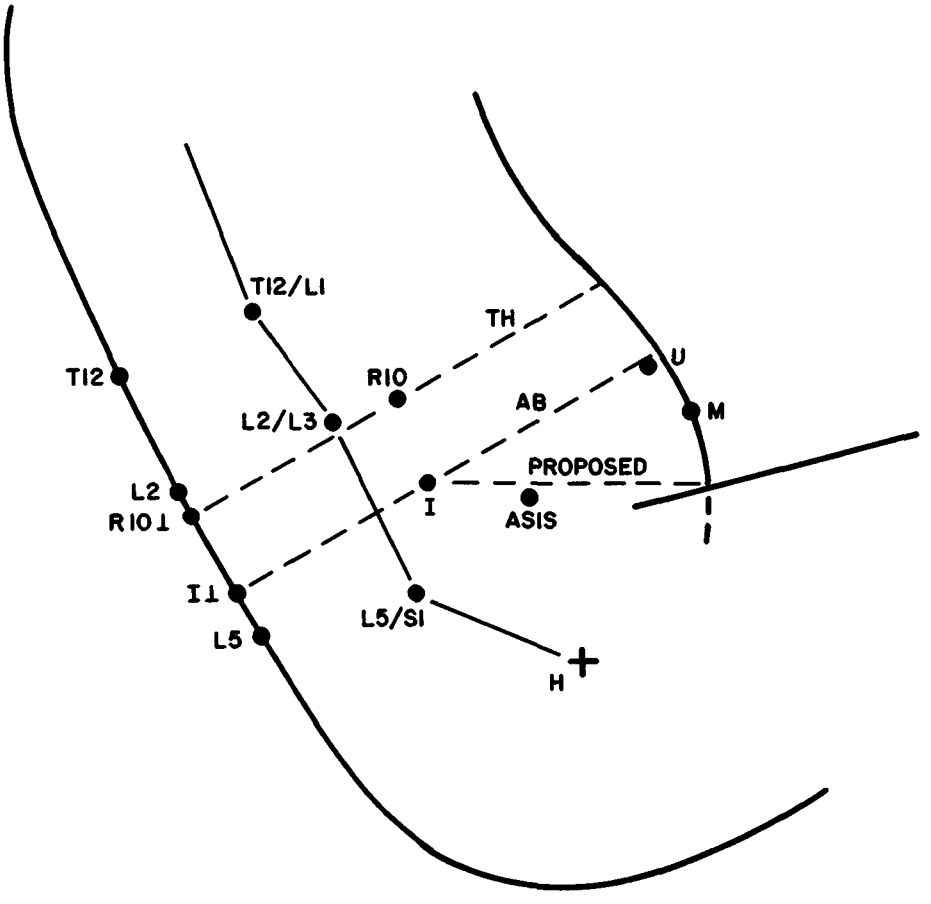

FIGURE 3. Construction of thorax and abdomen segmentation plane.

The conclusion was to present data based on a segmentation plane parallel to the thorax plane and recommend that new inertial and mass properties be developed based on the proposed definition given above and illustrated in Figure 3. The points used in the construction of the plane are:

Point	X_H (mm)	Y_H (mm)	Z_H (mm)
Iliocristale/Back Perpendicular	-188	0	35
Iliocristale	- 80	±161	93

The formula for the segmentation is:

$$.47312X_H - .88098Z_H + 119.78 = 0$$

The recommendation, then, is to use this formula until mass, center of gravity, and inertial properties can be measured directly from a solid casting of the surface form abdomen with the additional material from the pelvic region. Similar measurements would be required for the new pelvic region.

6.5 Hip Plane: First Attempt

The McConville et al. definition specifies that the plane "originates at the center of the crotch and passes laterally midway between the anterior-superior iliac spine and trochanter landmarks along the lines of the right and left inguinal ligaments." Construction of these planes thereby requires information on several features of the anatomy of the subject population.

From plots of data (Figure 4) and a review of pelvis and femur internal geometry, it appeared that a comparison should be made between the UMTRI trochanterion surface landmark obtained photographically and similar data obtained by other investigators. The torso-link data of Snyder et al. (1972) was gathered from a somewhat similar population (weight=175 pounds, height=70 inches). Seated measurements on these subjects show:

- Seat back to trochanter = 14.06 cm
- Seat surface to trochanter = 8.84 cm

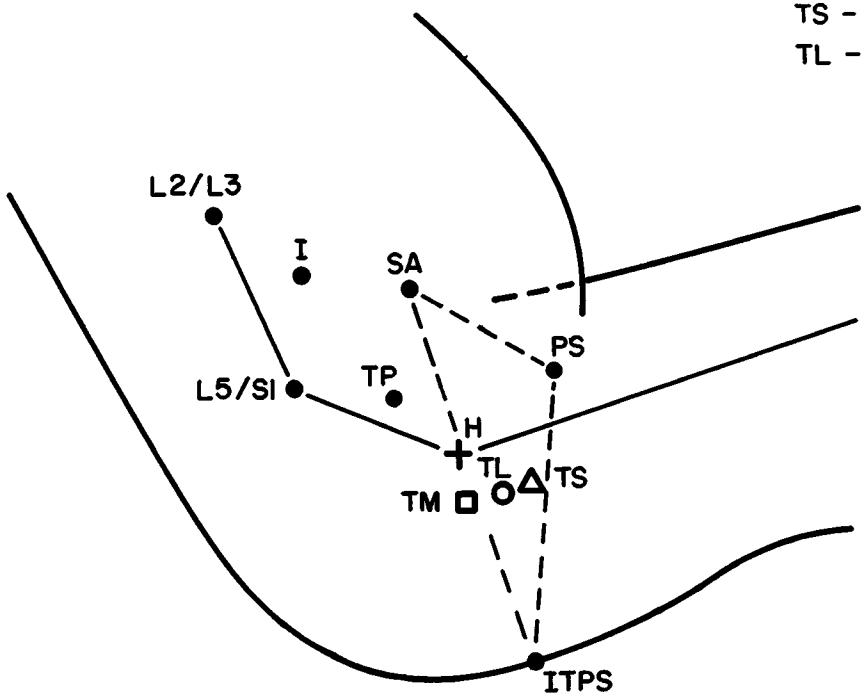

FIGURE 4. Construction of hip segmentation plane.

From the drawing of our somewhat more slumped subject and estimates of seat cushion and seat back lines, the trochanter landmark from photographic measurements yielded the following data using a similar measurement scheme:

- Seat back to trochanter = 12.1 cm
- Seat surface (deepest point) to trochanter = 14.7 cm

In order to obtain a further check on the location of this point, a mid-sized-male femur matching the average femur length of subjects in the UMTRI sample was set up in the lab to locate the pivot center in the acetabulum. The femur was oriented in space using the medial and lateral epicondyle point data and the center of the head of the femur (H-point). Using the McConville et al. definition of the trochanter landmark based on the most superior point (determined from the orientation of the femur in a standing subject), the trochanter landmark was found to be 5 mm forward and 25 mm down from the H-point. Using the present project definition of most lateral point, the trochanter landmark was found to be 35 mm forward and 12 mm down. The four versions are shown in Figure 4. The point estimate from the torso-link study falls between the values obtained from the skeletal reconstruction. In conclusion, a new point is defined called trochanterion (skeletal reconstruction) with the coordinates X_H=20, Y_H=±203, Z_H=-20. This will be used in all analyses which follow.

Although a point on the inguinal ligament line is well represented by the thigh/abdominal junction point (21, ±122, 81), it was not found possible to obtain realistic selection of a point representing the center of the crotch. Because three non-colinear points are required to construct a plane in three dimensions, the original hip plane concept used by McConville et al. was dropped.

6.6 Hip Plane: Successful Attempt

The objective of hip segmentation plane is to separate the upper leg region from the bony pelvis. The procedure used by Clauser et al. (1969) extended the plane "from the level of the iliac crest inferiorly along the external shelf of the ilium, cutting the rim of the

acetabulum and severing the ischial tuberosity (posteriorly at the level of the attachment of m. semimembranous, anteriorly at the mid-point of the ascending ramus of the ischium)." That procedure yields a plane which approximately bisects the H-point and removes as little of the bony pelvis as possible.

A procedure which defines a plane based on available data and which avoids cutting into the pelvic bone mass uses the four bony landmarks quantified by Reynolds et al. (1981):

Point	X_H (mm)	Y_H (mm)	Z_H (mm)
Anterior-Superior Iliac Spines	-25	±116	78
Pubotuberosity	34	± 25	29
Lateral Tuberosity Point	20	± 67	-55
Inferior Tuberosity Point	37	± 39	-61

To define a pelvic mass which is separate from the upper leg mass, a segmentation plane is proposed which does not intersect the average pelvis but which maintains the relation to the inguinal ligaments, is very similar to the other procedures, and can be quantified in three-dimensional coordinates.

To present pubotuberosity, a point 35 mm lateral to the pubic symphysis on (or near) the dummy surface has been selected. Likewise, for the anterior-superior iliac spine, a lateral shift of 10 mm from the surface marker is selected. The final point, which in some sense represents the bottom of the crotch, is selected as 10 mm lateral to and projected vertically to the seat surface from the inferior tuberosity point. These three points are:

Point	X_H (mm)	Y_H (mm)	Z_H (mm)
Pubotuberosity Surface	51	± 35	41
Shifted ASIS	-25	±126	83
Shifted Inferior Tuberosity	37	± 49	-107

The formula for the segmentation is:

$$-.76487X_H \pm .64407Y_H + .01143Z_H + 61.082 = 0$$

where the positive sign on Y_H is the right side of the body. This segmentation plane passes 8 mm lateral (oblique) to the H-point joint center and less than 2 mm from the lateral tuberosity.

6.7 Knee Plane

The McConville et al. definition specifies that the plane "passes through the lateral femoral epicondyle landmark parallel to the standing surface." Because of the difference between the standing and seated postures, this definition is not realistic. As an alternative, which is designed to separate the upper and lower leg masses, it is proposed to pass the plane through the lateral femoral epicondyles bisecting the angle in the X_HZ_H plane made by the lines connecting the upper and lower leg links. The plane is assumed to be parallel to the Y_H coordinate axis and has an angle of 14.56 degrees with respect to the vertical (Figure 5). Its formula is:

$$-.96788X_H + .25139Z_H + 358.59 = 0$$

The plane passes within 0.2 mm of the knee joint center.

6.8 Ankle Plane

The McConville et al. definition specifies that the plane "originates at the sphyrion landmark and passes through the ankle parallel to the standing surface." This plane is maintained fairly well by constructing a plane through the sphyrion, parallel to the Y_H axis, and perpendicular to a line connecting the knee and ankle joints projected into the X_HZ_H plane. Its angle with the vertical is 42.35 degrees and the formula is:

$$.73904X_H - .67366Z_H - 605.88 = 0$$

6.9 Shoulder Plane

The McConville et al. definition specifies that the plane "originates at the acromion landmark and passes downward through the anterior and posterior scye creases at the level of the axilla." This

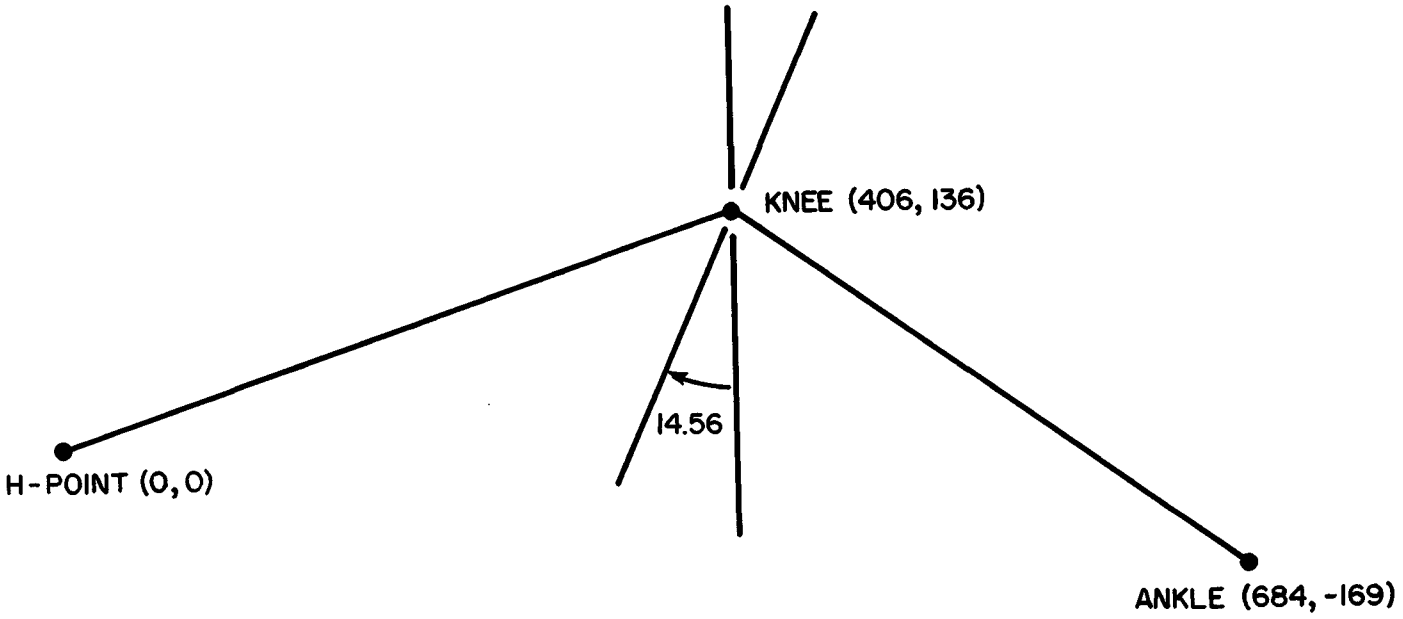

FIGURE 5. Construction of knee segmentation plane.

segmentation plane appears to be similar for both the standing and seated postures. The three points needed for its definition are:

Point	X_H (mm)	Y_H (mm)	Z_H (mm)
Acromion	-224	±203	419
Anterior Scye	- 97	±154	380
Posterior Scye	-214	±197	306

The formula for this segmentation is:

$$.35502X_H \pm .93466Y_H - .01821Z_H - 102.58 = 0$$

where the plus sign on Y_H refers to the left side of the body. The distance of this plane from the glenohumeral joint center is estimated to be proximal by 14 mm while the distance to the claviscapular joint is estimated to be even larger at 35 mm. It is recommended that this segmentation procedure be evaluated carefully during an overall review of the definition of the entire shoulder girdle (Section 9).

6.10 Elbow Plane

The McConville et al. definition specifies that the plane "originates at the olecranon landmark and passes through the medial and lateral humeral epicondyle landmarks." This definition appears to be satisfactory. The three points needed for definition are:

Point	X_H (mm)	Y_H (mm)	Z_H (mm)
Olecranon	53	±210	186
Medial Humeral Epicondyle	32	±173	199
Lateral Humeral Epicondyle	32	±242	224

The formula for the segmentation is:

$$-.96349X_H \pm .22Y_H - .60719Z_H + 107.2 = 0$$

where the plus sign on Y_H refers to the left side of the body. The plane passes about 3 mm from the estimated joint center for the seated posture.

7.0 DEVELOPMENT OF ANATOMICALLY BASED SEGMENT COORDINATE SYSTEMS

This section shows the development of anatomically based coordinate systems for each of the various segments of the body. The coordinate systems which have been constructed are the same, or very similar to, those which have been reported by McConville et al. (1980) in developing anthropometric relationships of body and body segment moments of inertia. As such, they will be used directly in the presentation of center of mass and inertial data and will provide the linkage between the coordinate systems defining the principal axes of inertia and the standard coordinate system at the H-point center.

In order to construct coordinate systems and relate them to the standard system, it is necessary to know three points in the segment. For most of the present analyses, this is done by selecting one point at the origin, a second point on an axis, and the third point in one of the orthogonal planes. The sub-sections that follow identify the points required, discuss necessary details of the construction, and present results as direction cosine matrices for transforming from anatomical to standard coordinates.

The subscript A is used to denote anatomical coordinate systems. It should be noted that there is a different anatomical coordinate system for each segment and more subscripts could be added to represent each specific anatomical system. However, it is felt that this additional cumbersome notation is unnecessary due to the context in which the symbols are used.

7.1 Head Axis System

The McConville et al. definition for the head axis system is as follows:

- X_AY_A Plane: Right and left tragion and right infraorbitale
- Y_AZ_A Plane: Right and left tragion
- X_AZ_A Plane: Sellion

7.0 DEVELOPMENT OF ANATOMICALLY BASED SEGMENT COORDINATE SYSTEMS

This section shows the development of anatomically based coordinate systems for each of the various segments of the body. The coordinate systems which have been constructed are the same, or very similar to, those which have been reported by McConville et al. (1980) in developing anthropometric relationships of body and body segment moments of inertia. As such, they will be used directly in the presentation of center of mass and inertial data and will provide the linkage between the coordinate systems defining the principal axes of inertia and the standard coordinate system at the H-point center.

In order to construct coordinate systems and relate them to the standard system, it is necessary to know three points in the segment. For most of the present analyses, this is done by selecting one point at the origin, a second point on an axis, and the third point in one of the orthogonal planes. The sub-sections that follow identify the points required, discuss necessary details of the construction, and present results as direction cosine matrices for transforming from anatomical to standard coordinates.

The subscript A is used to denote anatomical coordinate systems. It should be noted that there is a different anatomical coordinate system for each segment and more subscripts could be added to represent each specific anatomical system. However, it is felt that this additional cumbersome notation is unnecessary due to the context in which the symbols are used.

7.1 Head Axis System

The McConville et al. definition for the head axis system is as follows:

- X_AY_A Plane: Right and left tragion and right infraorbitale
- Y_AZ_A Plane: Right and left tragion
- X_AZ_A Plane: Sellion

Coordinates for the three points for the head axis system are:

Point	X_H (mm)	Y_H (mm)	Z_H (mm)
Infraorbitale (R)	- 96	- 34	620
Tragion (L)	-185	83	614
Tragion (R)	-185	- 83	614

The origin of the coordinate system is at the center of a line connecting the tragions. In lab coordinates the point is:

$$X_H=-185,\ Y_H=0,\ Z_H=614$$

The origins of all segment coordinate systems are summarized in Table 6. The direction cosine matrix for the transformation from laboratory into head segment coordinates is given in Table 7 (degrees) and Table 8 (cosine of angle).

TABLE 6

LOCATION OF ORIGINS OF SEGMENT ANATOMICAL COORDINATE SYSTEMS

Segment	X_H (mm)	Y_H (mm)	Z_H (mm)
Head	-185	0	614
Neck	-266	0	489
Thorax	-209	0	71
Abdomen	- 93	0	133
Pelvis	- 25	0	83
Upper Arms	-224	+203*	419
Lower Arms	46	±243	209
Upper Legs	20	±203	- 20
Lower Legs	424	± 88	128
Feet	796	±126	- 96

*The positive sign on Y_H refers to the left side of the body.

TABLE 7

ANATOMICAL AXES WITH RESPECT TO HIP POINT AXIS SYSTEM
(Cosine Matrix Expressed in Degrees)

Segment		X_H	Y_H	Z_H
Head	X_A	3.86	90.	86.14
	Y_A	90.	0.	90.
	Z_A	93.86	90.	3.86
Neck	X_A	20.8	90.	110.8
	Y_A	90.	0.	90.
	Z_A	69.2	90.	20.8
Thorax	X_A	7.8	90.	82.2
	Y_A	90.	0.	90.
	Z_A	97.8	90.	7.8
Abdomen	X_A	28.1	90.	61.9
	Y_A	90.	0.	90.
	Z_A	118.1	90.	28.1
Pelvis	X_A	61.05	90.	28.96
	Y_A	90.	0.	90.
	Z_A	151.04	90.	61.05
Upper Arm (L)	X_A	52.5	105.7	41.8
	Y_A	85.8	17.2	73.3
	Z_A	142.2	96.9	53.0
Upper Arm (R)	X_A	52.5	74.3	41.8
	Y_A	94.2	17.2	106.7
	Z_A	142.2	83.1	53.0
Lower Arm with Hand (L)	X_A	128.2	71.4	44.1
	Y_A	68.6	22.2	95.6
	Z_A	134.1	78.4	133.5
Lower Arm with Hand (R)	X_A	128.2	108.6	44.1
	Y_A	111.4	22.2	84.4
	Z_A	134.1	101.6	133.5
Upper Leg (L)	X_A	110.9	83.8	21.9
	Y_A	86.0	6.3	95.1
	Z_A	158.8	88.1	111.2
Upper Leg (R)	X_A	110.9	96.2	21.9
	Y_A	94.0	6.3	84.9
	Z_A	158.8	91.9	111.2

TABLE 7
ANATOMICAL AXES WITH RESPECT TO HIP POINT AXIS SYSTEM
(Cosine Matrix Expressed in Degrees, Continued)

Segment		X_H	Y_H	Z_H
Lower Leg (L)	X_A	46.2	67.6	52.2
	Y_A	103.5	22.9	108.0
	Z_A	133.1	85.9	43.3
Lower Leg (R)	X_A	46.2	112.4	52.2
	Y_A	76.5	22.9	72.0
	Z_A	133.1	94.1	43.3
Foot (L)	X_A	59.9	78.4	32.7
	Y_A	90.	13.4	103.4
	Z_A	149.9	83.3	60.8
Foot (R)	X_A	59.9	101.6	32.7
	Y_A	90.	13.4	76.6
	Z_A	149.9	96.7	60.8

TABLE 8

ANATOMICAL AXES WITH RESPECT TO HIP POINT AXIS SYSTEM
(Cosine Matrix)

Segment		X_H	Y_H	Z_H
Head	X_A	.998	0.	.0673
	Y_A	0.	1.	0.
	Z_A	-.0673	0.	.998
Neck	X_A	.935	0.	-.355
	Y_A	0.	1.	0.
	Z_A	.355	0.	.935
Thorax	X_A	.991	0.	.136
	Y_A	0.	1.	0.
	Z_A	-.136	0.	.991
Abdomen	X_A	.882	0.	.471
	Y_A	0.	1.	0.
	Z_A	-.471	0.	.882
Pelvis	X_A	.484	0.	.875
	Y_A	0.	1.	0.
	Z_A	-.875	0.	.484
Upper Arm (L)	X_A	.609	-0.270	.746
	Y_A	.0728	0.955	.287
	Z_A	-.790	-0.120	.602
Upper Arm (R)	X_A	.609	0.270	.746
	Y_A	-.0728	0.955	.287
	Z_A	-.790	0.120	.602
Lower Arm with Hand (L)	X_A	-.618	0.319	.718
	Y_A	.365	0.926	-.0982
	Z_A	-.697	0.201	-.689
Lower Arm with Hand (R)	X_A	-.618	-0.319	.718
	Y_A	-.365	0.926	.0982
	Z_A	-.697	-0.201	-.689
Upper Leg (L)	X_A	-.356	0.108	.928
	Y_A	.0705	0.994	-.0884
	Z_A	-.932	0.0340	-.362
Upper Leg (R)	X_A	-.356	-0.108	.928
	Y_A	-.0705	0.994	.0884
	Z_A	-.932	-0.0340	-.362

TABLE 8
ANATOMICAL AXES WITH RESPECT TO HIP POINT AXIS SYSTEM
(Cosine Matrix, Continued)

Segment		X_H	Y_H	Z_H
Lower Leg (L)	X_A	.692	0.382	.612
	Y_A	-.234	0.922	-.310
	Z_A	-.683	0.0709	.727
Lower Leg (R)	X_A	.692	-0.382	.612
	Y_A	.234	0.922	.310
	Z_A	-.683	-0.0709	.727
Foot (L)	X_A	.501	0.200	.842
	Y_A	0.	0.973	-.232
	Z_A	-.865	0.116	.487
Foot (R)	X_A	.501	-0.200	.842
	Y_A	0.	0.973	.232
	Z_A	-.865	-0.116	.487

It is now possible to compare McConville et al. surface landmark locations reported in segment coordinates with similar surface landmarks measured at UMTRI. The X_A distance from tragion to infraorbitale is 72.3 mm for McConville et al. and 89 mm for UMTRI which is clearly a large discrepancy. A check of Churchill and Truett (1957) data show subtracting "external canthus to wall" from "tragion to wall" yields 63 mm. That value is comparable to the McConville et al. data. To further study the issue, head-size data such as length and circumference were checked and found very comparable as shown below:

Point	McConville et al. 1980	UMTRI 1983
Head Length (mm)	199.3	197.4
Head Circumference (mm)	572.7	570.6

Because of this similarity, the discrepancy is assumed to be in tragion location. The origin of coordinates is selected to be between the UMTRI tragions as indicated previously.

Figure 6 shows the head anatomical coordinate system. The McConville et al. coordinate system is superimposed with the infraorbitales coincident and the tragions located along the X_A axis. In this presentation, the center of volume, as specified in the McConville et al. system, lies 8.5 mm behind and 31.3 mm above the McConville et al. origin and at the same time is 8.4 mm in front of and 31 mm above the UMTRI origin. The relationship of origin to center of volume in the UMTRI definition is closer to that of Beier et al. (1980). Because of the overall head dimensional similarity (e.g., length, breadth, circumference), it is felt that the above analysis is a reasonable approximation for the various data resources.

7.2 Neck Axis System

The McConville et al. definition for the neck axis system is as follows:

- X_AZ_A Plane: Adam's apple, cervicale, suprasternale
- X_AY_A Plane: Including a line in the X_HZ_H plane connecting the cervicale with the midpoint of a line connecting the clavicales
- Y_AZ_A Plane: Cervicale

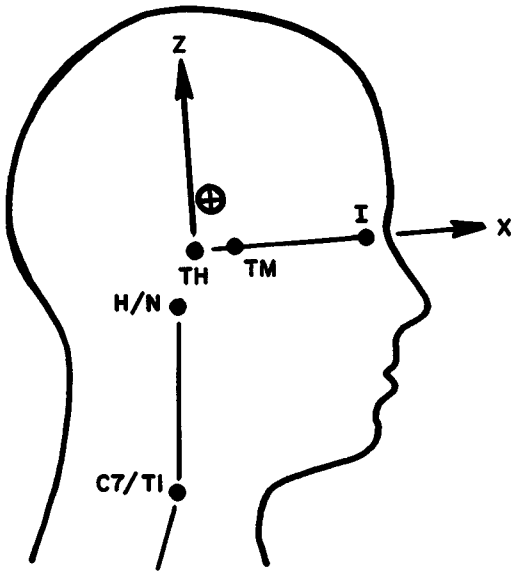

CODE

JOINTS (H/N, C7/TI)

⊕ - HEAD CENTER OF GRAVITY

I - INFRAORBITALE (UMTRI AND McCONVILLE SUPERIMPOSED)

TM - McCONVILLE TRAGION

TH - UMTRI TRAGION

FIGURE 6. Head anatomical coordinate system.

The three points required are:

Point	X_H (mm)	Y_H (mm)	Z_H (mm)
Cervicale	-266	0	489
Clavicale (L)	-145	23	443
Clavicale (R)	-145	- 23	443

Because of the symmetry assumption, it is not necessary to provide coordinates for Adam's apple or suprasternale. The origin of the coordinate system is at the cervicale:

$$X_H=-266,\ Y_H=0,\ Z_H=489$$

The direction cosine matrix for the transformation is given in Tables 7 and 8.

7.3 Thorax Axis System

The McConville et al. definition of the thorax axis system is as follows:

- X_AZ_A Plane: Suprasternale, cervicale, and mid-spine at level of 10th rib
- Y_AZ_A Plane: Cervicale and 10th rib level at mid-spine
- X_AY_A Plane: 10th rib level at mid-spine

The symmetry assumption reduces the requirements to the points defining the Y_AZ_A and X_AY_A planes. The "10th rib level at mid-spine" point is not applicable to the seated position (see Section 6.3). In order to approximate this point for a seated posture, a line was constructed from the 10th rib landmark which was perpendicular to a line connecting the T12 and L5 surface landmarks. In other words, a line was constructed which was perpendicular to an approximation of the seat back line. The point which was selected to replace the McConville et al. point is called the R10/back perpendicular point and is the intersection of the perpendicular line with the line connecting the T12 and L5 surface

landmarks. The points needed for constructing the transformation are thus:

Point	X_H (mm)	Y_H (mm)	Z_H (mm)
Cervicale	-266	0	489
R10/Back Perpendicular	-209	0	71

The origin of coordinates is at the R10/back perpendicular point and the direction matrix for the transformation is given in Tables 7 and 8.

7.4 Abdomen Axis System

The McConville et al. definition for the abdomen axis system is as follows:

- X_AY_A Plane: Right and left 10th rib and at mid-spine at level of 10th rib
- Y_AZ_A Plane: Right and left 10th rib
- X_AZ_A Plane: 10th rib mid-spine

Again the "mid-spine at level of 10th rib" point is not applicable to the seated posture. The R10/back perpendicular point, discussed in Section 7.3, is again used as a substitute. The points needed for construction of the transformation are:

Point	X_H (mm)	Y_H (mm)	Z_H (mm)
R10/Back Perpendicular	-209	0	71
10th Rib (L)	- 93	156	133
10th Rib (R)	- 93	-156	133

The origin of coordinates is at the center of a line connecting the right and left 10th rib surface landmarks:

$$X_H=-93,\ Y_H=0,\ Z_H=133.$$

The direction cosine matrix for the transformation is given in Tables 7 and 8.

7.5 Pelvis Axis System

The McConville et al. definition of the pelvis axis system is as follows:

- Y_AZ_A Plane: Right left anterior-superior iliac spines and and symphysion
- X_AY_A Plane: Right and left anterior-superior iliac spines
- X_AZ_A Plane: Mid-spine at level of posterior-superior iliac spine

The body symmetry assumption eliminates the need for the mid-spine at level of posterior-superior iliac spine point. Remaining are definitions of symphysion and anterior-superior iliac spine. Four different axis systems for the pelvis are used at various places in this report. The first is the laboratory system based on the standard seat. The second is that of McConville et al. which is used for mass and inertial property definition. The third is that of Reynolds et al., used in the study of the spatial geometry of the pelvic bone, and the fourth is the UMTRI pelvis segment axis system. As a result, three sets of definitions should be compared, those of McConville et al. (1980), Reynolds et al. (1981), and the present UMTRI study. They are:

Symphysion

McConville et al. 1980: "The lowest point on the superior border of the pubic symphysis, the anterior juncture of the pelvic bones."

Reynolds et al. 1981: "The midpoint of a line between point 180, right superior pole, pubic symphysis, and point 183, left superior pole, pubic symphysis..." Point 180 is "at the intersection of the longitudinal midline axis of the pubic symphysis with the superior margin of the symphyseal face of the right innominate bone."

UMTRI 1983: "The superior margin of the pubic symphysis in the midline" (i.e. pelvic crest).

Anterior-Superior Iliac Spine

McConville et al. 1980: "The most prominent point on the anterior-superior spine of the ilium."

Reynolds et al. 1981: "Left iliospinale, summum, 201-203: The left innominate rests on its medial surface with the iliac blade and pubic symphysis in contact with the horizontal surface of an osteometric board. Move the bone into the right angle corner of the board in such a way that the superior border of the iliac crest in contact with the vertical plate ..."

UMTRI 1983: "The most prominent point on the anterior-superior spine of the left ilium."

With respect to both points, the McConville et al. and UMTRI definitions refer to surface landmarks while Reynolds et al. refers directly to the skeleton. In comparing the definitions, the attempt was made to visualize the Reynolds et al. quantities as if tissue were in place over the bone. From this point of view, the symphysion targets of UMTRI and Reynolds et al. appear to be directed at approximately the same point while the McConville et al. definition is a bit more anterior. It is estimated that the difference is less than one centimeter. For the anterior-superior iliac spines, the McConville et al. and UMTRI definitions are identical. The Reynolds et al. definition, which is more precise in an absolute measurement sense, appears to define a very similar point to the other two.

The origin of coordinates in the three segment coordinate systems is based on the midpoint of a line connecting the anterior-superior iliac spines. As these points are defined to be nearly the same (assuming the tissue thickness shift for the Reynolds et al. system is valid), then the origins are assumed to coincide (with the Reynolds et al. system based on the related skeletal landmarks under the surface of the skin). The symphysion is used to construct an axis direction in the three cases. The slight difference in the McConville et al. definition is believed to be within the error bounds of the measurements but should ultimately be evaluated using the concepts suggested by Robbins (1977) in a brief study of errors in definition of an anatomically based coordinate system using anthropometric data.

The previous discussion shows a procedure for merging the data bases of UMTRI, McConville et al., and Reynolds et al. The results have already been used in establishment of a standard seat coordinate system

(Section 4). They were used in Section 9 to locate the hip and lumbar-spinal (L5/S1) joints based on Reynolds et al. work. They are used here to obtain a transformation to segment coordinates in order to utilize the pelvic mass and inertial data of McConville et al.

The three points needed for construction of the transformation are:

Point	X_H (mm)	Y_H (mm)	Z_H (mm)
ASIS (L)	-25	116	83
ASIS (R)	-25	-116	83
Symphysion	51	0	41

The origin of the anatomical system is at:

$$X_H=-25,\ Y_H=0,\ Z_H=83$$

The direction cosine matrix for the transformation is given in Tables 7 and 8.

7.6 Upper Arm Axis System

The McConville et al. definition for the upper arm axis system is as follows:

- Y_AZ_A Plane: Acromion as well as medial and lateral humeral epicondyles
- X_AZ_A Plane: Lateral humeral epicondyle and acromion
- X_AY_A Plane: Acromion

This axis system is not consistent with body mobility as the acromion is not part of the arm link. The axis system migrates as the arm rotates. With respect to the standing position, in which the McConville et al. data were developed, the anatomical long axis is approximately along the axis of the humerus. In forward reach, however, the axis from acromion to humeral epicondyles is above the axis of the humerus.

In the case of the seated occupant shown in Figure 1, it is seen that the upper arm is rotated less than 20 degrees from the torso long

axis. Therefore, for the present estimates of center of mass and inertial properties, the McConville et al. definition is assumed to be adequate. These basic properties probably will not vary much with arm rotation whereas the anatomical axis definition is totally inadequate for arm mobility studies.

The points needed for construction of the transformations are:

Point	X_H (mm)	Y_H (mm)	Z_H (mm)
Acromion (L and R)	-224	±203	419
Lateral Humeral Epicondyle (L and R)	32	±242	224
Medial Humeral Epicondyle (L and R)	32	±173	199

The origins of coordinates for the two segments are at the acromions:

$$X_H=-224,\ Y_H=\pm 203,\ Z_H=419$$

where the positive sign on Y_H refers to the left side of the body. The direction cosine matrices for both left and right upper arms are given in Tables 7 and 8.

7.7 Lower Arm Axis System (Hands Included)

The McConville et al. definition for the lower arm axis system is as follows:

- Y_AZ_A Plane: Distal end of ulnar and radial styloid processes and radiale
- X_AZ_A Plane: Distal end of ulnar styloid process and radiale
- X_AY_A Plane: Radiale

The points needed for construction of the transformations are:

Point	X_H (mm)	Y_H (mm)	Z_H (mm)
Radiale (L and R)	46	±243	209
Ulnar Styloid (L and R)	226	±191	387
Radial Styloid (L and R)	211	±135	399

The origins of coordinates for the two segments are at the radiales as given. The direction cosine matrices for both left and right lower arms are given in Tables 7 and 8.

7.8 Upper Leg (Complete Up to Pelvis) Axis Systems

The McConville et al. definition for the upper leg axis system is as follows:

- $Y_A Z_A$ Plane: Trochanterion as well as right and left lateral femoral epicondyles
- $X_A Z_A$ Plane: Lateral femoral epicondyles and trochanterion
- $X_A Y_A$ Plane: Trochanterion

The points needed for construction of the transformation are:

Point	X_H (mm)	Y_H (mm)	Z_H (mm)
Trochanterion (skeletal reconstruction, L and R)	20	±203	- 20
Lateral Femoral Epicondyle (L and R)	404	±189	127
Medial Femoral Epicondyle (L and R)	407	± 87	142

The point trochanterion (skeletal reconstruction) was defined and developed in Section 6.5 of this report. The origins of coordinates for the two segments are at trochanterions (skeletal reconstruction) as given. The direction cosine matrices for both left and right upper legs are given in Tables 7 and 8.

In order to compare the geometry of the upper legs using the McConville et al. and UMTRI data bases, the distance from trochanterion to femoral epicondyles was computed. The UMTRI leg appeared to be about 20 mm short. However, the two studies palpated different points on the trochanter (Section 6.5). When this is taken into account, there is only about 10 mm difference between the two studies which is estimated to be quite reasonable given the experimental difficulties with trochanterion.

7.9 Lower Leg Axis Systems

The McConville et al. definition for the lower leg axis system is as follows:

- $Y_A Z_A$ Plane: Tibiale, sphyrion, lateral malleolus
- $X_A Z_A$ Plane: Sphyrion and tibiale
- $X_A Y_A$ Plane: Tibiale

The points needed for construction of the transformation are:

Point	X_H (mm)	Y_H (mm)	Z_H (mm)
Tibiale (L and R)	424	± 88	128
Sphyrion (L and R)	684	±61	-149
Lateral Malleolus (L and R)	680	±126	-185

The origins of coordinates for the two segments are at tibiale as given above. The direction cosine matrices for both left and right lower legs are given in Tables 7 and 8.

7.10 Feet Axis Systems

The McConville et al. definition for the feet axis systems is as follows:

- $X_A Y_A$ Plane: Metatarsal/phalangeal I and V landmarks and posterior calcaneus
- $X_A Z_A$ Plane: Tip of digit II and posterior calcaneus
- $Y_A Z_A$ Plane: Metatarsal/phalangeal I

The posterior calcaneus is estimated to coincide with the heel point on the standard seat buck. Using the data of McConville et al. and the relationship between the four points required for construction of the system, an anatomical origin was computed. This point was combined with two others, as follows, to construct the transformation:

Point	X_H (mm)	Y_H (mm)	Z_H (mm)
Constructed Origin (L and R)	796	±126	- 96
Metatarsal/Phalangeal I (L and R)	796	± 84	-86
Heel Point (L and R)	705	± 94	-250

The direction cosine matrices for both left and right feet are given in Tables 7 and 8.

8.0 VOLUME, MASS, AND INERTIAL PROPERTIES

The volume, mass, and inertial properties are based on the results of McConville et al. 1980. For each of the segments the following data are provided:

- Anthropometry of segment (means)
- Volume (mean values and regression equations using anthropometric measures)
- Center of volume from anatomical axis origin
- Principal moments of inertia (mean values and regression equations using anthropometric measures)
- Principal axes of inertia with respect to anatomical axes

The following four subsections of this report compare the basic anthropometric properties of the UMTRI-seated and Air-Force-standing populations, develop the volume and mass properties of the body segments, present centers of gravity based on center of volume, and tabulate the inertial properties and principal axes.

8.1 Basic Anthropometric Properties of Each Segment

For each body segment a variety of anthropometric measurements were taken in both the McConville et al. study and the present one at UMTRI. One of the uses of these data is in regression equations for segment volume and inertial properties. As such, they will be discussed and compared in some detail. The measurements made at UMTRI were taken in the vehicle seated posture, where possible, whereas the standard standing position was used in the previous work. The following text compares the anthropometry and discusses the effects that differences might have on segment shape. It should be noted that the comparable statures and weights are:

Quantity	McConville et al. (1980)	UMTRI
Stature (mm)	1774.9	1751.4
Weight (lbs)	170.4	168.8

For the head, data from the two studies are as follows:

Quantity	McConville et al. (1980)	UMTRI
Head Length	199.3	197.4
Head Breadth	153.2	158.0
Head Circumference	572.7	570.6
Head Height	166.5	230.9

These measurements are very comparable, except for head height, and can be used directly in regression equations. In the original data it was defined as the difference between stature and mastoid heights while at UMTRI it was taken as the distance from the bottom of the chin to the highest point on the top of the head.

For the neck, data from the two studies are as follows:

Quantity	McConville et al. (1980)	UMTRI
Neck Circumference	376.7	388.2
Neck Breadth	122.9	118.0
Neck Length	81.8	84.8

These measurements are very comparable. The UMTRI breadth and circumference data are based on the average of measurements taken at two heights along the neck.

For the thorax, data from the two studies are as follows:

Quantity	McConville et al. (1980)	UMTRI Standing	UMTRI Seated
Chest Circumference	965.1	961	1009.6
Chest Breadth	331.9		348.7
Thorax Length	403.1		(355,390,415)
10th Rib Breadth	298.5		
10th Rib Circumference	821.5		909.4

The basic data demonstrate a considerable difference between the seated and standing postures. The segmentation plane at the neck is horizontal for both postures whereas the front of the thorax segmentation plane has

been tilted upward to maintain an orientation approximately perpendicular to the seatback. The three numbers given for UMTRI (seated) thorax length were determined as follows:

- Vertical distance from neck segmentation plane to 10th rib landmark
- Direct distance from cervicale to 10th rib landmark
- Vertical distance from neck segmentation plane to 10th rib perpendicular intersection with seat back

That this redirection of the thorax segmentation plane and compressing of the abdominal and lower thoracic contents actually takes place appears to be verified by the increased chest circumference and breadth in the seated posture. The measure of thorax length in the standing posture (403.1 mm) is not too different from the distance along the seated spinal linkage from cervicale to the 10th rib landmark (390 mm). The curving of the spine in the seated posture does tend to compress the frontal abdominal and thorax region as indicated by the shorter thorax length obtained by using a parallel through the 10th rib landmark (355 mm). This will tend to move the center of gravity forward in the thorax as the seated posture is assumed. Because the curving of the spine tends to move the thorax segment Z_A axis further toward the front of the body than is the case with the McConville et al. axis, it will be assumed that this tends to compensate. (This can be visualized by connecting cervicale and R10/back perpendicular landmarks as has been done in Figure 7.) It should also be noted that the thorax segment X_A axis is placed further below the abdomen segmentation plane than in the McConville et al. case. This should tend to compensate for spreading of tissue toward the bottom of the thorax. The term "compensation" is used to reflect that the center of gravity will be moved around in the segment depending on the placement of segment coordinate axes.

In conclusion, the center of mass location will be conditionally accepted. In order to improve upon these data, a casting of the thorax segment should be made so that improved center-of-gravity and inertial properties can be measured directly as there is no easy computational procedure except for the photographic and analytical methods reported by McConville et al.

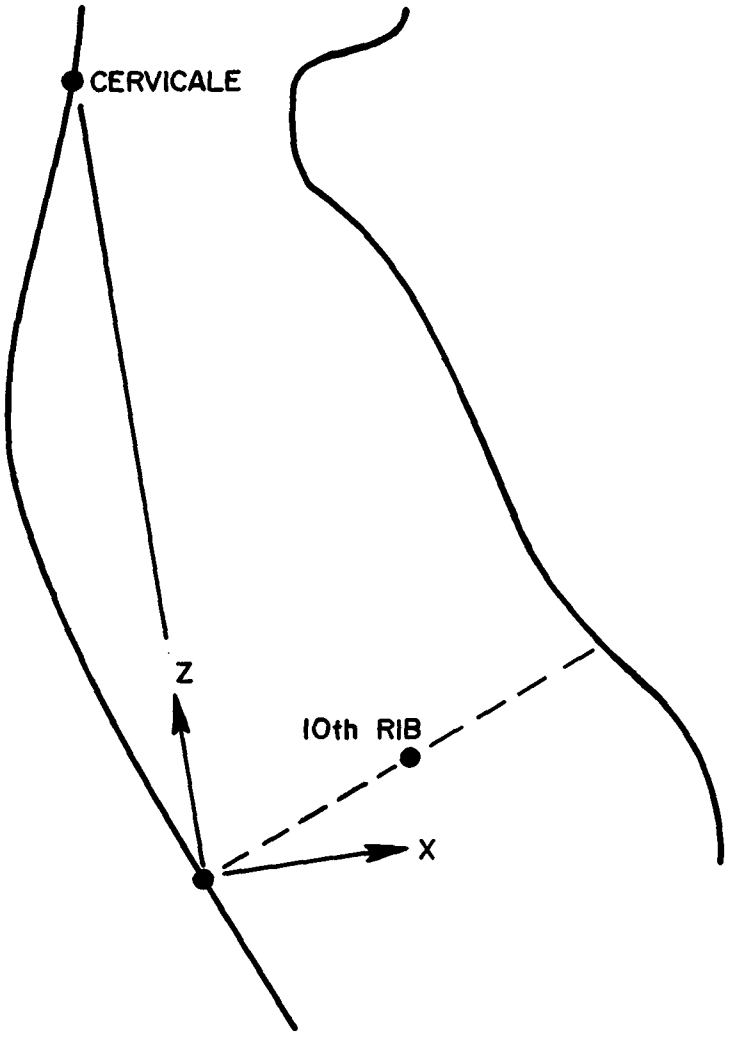

FIGURE 7. Segment axes in thorax for seated posture.

For the abdomen, data from the two studies are as follows:

Quantity	McConville et al. (1980)	UMTRI Standing	UMTRI Seated
Abdomen Length	50.1		42.0
Waist Circumference	857.0	859.0	903.8
10th Rib Breadth	298.5		
10th Rib Circumference	821.5		909.4
Waist Breadth	312.3		313.5
Suprailiac Skinfold	152.4	210.9	

The major feature of this comparison is that the abdominal segment is thinner and has a greater circumference. This is caused by the curving of the spine as the pelvis rotates upward toward the rib cage during the process of sitting down in a car seat. A qualitative pilot study at UMTRI involving a targeted subject in both seated and standing postures yielded this same conclusion regarding the narrowing of the abdominal area. Section 6.4 of this report presented a recommendation for a different segmentation and delineation of the abdominal area which better defines the extent of the soft abdomen. Although data based on McConville et al. are being used in this volume, it is strongly recommended, as was done for the thorax, that castings of the proposed abdominal segment be made so that revised mass and inertial properties can be directly determined.

For the pelvis, data from the two studies are as follows:

Quantity	McConville et al. (1980)	UMTRI Standing	UMTRI Seated
Buttock Circumference	952.9	944.4	
Buttock Depth	240.8		220-255
Bispinous Breadth	222.9	224.6	
Pelvic Length	258.3		235
Hip Breadth (maximum)	346.2		384.7
Suprailiac Skinfold	152.4	210.9	

There are several differences between the data which appear to be related to postural differences. The UMTRI measure reported as buttock circumference is hip circumference (maximum). Representative buttock

depths can be selected by measuring the perpendicular distance to the seat back from anatomical landmarks. These distances range from about 220 mm at the pubic symphysis to about 255 mm at the point of maximum abdominal protrusion. It is therefore assumed that the McConville et al. value (240.8) is a rough measure of this quantity. Pelvic length is defined by McConville et al. as the difference between gluteal furrow height and iliocristale height. An UMTRI estimate for this quantity is the perpendicular distance from iliocristale to the seat surface. This perpendicular line is essentially parallel to the seat back. The pelvic length, although not strictly comparable, is smaller for the seated subject perhaps due to the compression of tissue during the seating process. Also, the seated hip breadth is larger as would be expected from tissue being displaced toward the side of the subject/seat interface during the seating process. Because the pelvic mass is to a great extent determined by the shape and extent of the bony pelvis, the mass and inertial properties will be computed based on the McConville et al. data. Some corrections are suggested by using the UMTRI modified anthropometric constructions just presented. If the proposed new segmentation plane for the abdomen is accepted, then it is recommended that a casting be made of the new pelvic mass in order to obtain data for revised properties.

For the upper arms, data from the two studies are as follows:

Quantity	McConville et al. (1980)	UMTRI Standing	UMTRI Seated
Axilla Arm Circumference	319.1		
Biceps Circumference Relaxed	299.7	298.6	
Biceps Circumference Flexed	321.0		314.6
Acromion-Radiale Length	333.9	329.0	
Elbow Circumference	265.7		285.3
Biceps Depth Relaxed	108.3		108.
Elbow Breadth	70.7		80.2
Biceps Skinfold	37.4		
Triceps Skinfold	94.4	100.4	
Axilla Arm Depth	124.9		

These measures are quite similar with the exceptions of elbow circumference which becomes larger as the elbow flexes and elbow breadth

which was measured across soft tissue for the UMTRI subjects. In the regression equations, the biceps circumference flexed data from UMTRI are substituted for axilla arm circumference in that the biceps are not flexed much in the driving posture. Also, the McConville et al. data for axilla arm depth are used.

For the lower arms (hands included), data from the two studies are as follows:

Quantity	McConville et al. (1980)	UMTRI Standing	UMTRI Seated
Elbow Circumference	265.7		285.3
Midforearm Breadth	79.5		82.0
Midforearm Circumference	234.2	253.7	182.5-275.3
Wrist Circumference	169.9		168.7
Hand Length	189.4	187.2	
Hand Breadth	86.4	85.3	
Hand Circumference	208.7		
Forearm-Hand Length	459.8	474.0	

In most of the cases, similar, but not precisely the same, measurements were available for the two groups of subjects. The elbow circumference is larger due to flexion in the seated position. There was no equivalent measurement for midforearm circumference as UMTRI reported the minimum and maximum values given in the table. The forearm-hand length was measured with the arm flexed at 90 degrees for the UMTRI subjects while McConville et al. added radiale-stylion length to hand length.

For the upper legs, data from the two studies are as follows:

Quantity	McConville et al. (1980)	UMTRI Standing	UMTRI Seated
Thigh Length	465.5	435.3	447.1
Upper Thigh Circumference	570.2		578.6
Mid Thigh Circumference	529.0	515.1	503.5
Mid Thigh Depth	174.0		148.
Knee Circumference	374.1		392.2
Knee Breadth	96.1		101.3
Gluteal Furrow Depth	193.8		184.

Thigh length is represented differently in the two studies. UMTRI uses trochanterion to lateral femoral epicondyle while McConville et al. reports tibiale to trochanterion. As the femoral epicondyle is a landmark associated with the upper leg link and closely correlated with the knee joint center, the UMTRI values will be used. Mid thigh depth is estimated as the distance from the top of the thigh to the seat surface and thus is smaller for the UMTRI sample. The knee measurements are undoubtedly larger based on the movement of tendons during knee flexion. All in all, the data appear sufficiently alike to warrant use of the McConville et al. data base. In summary, the overall shape changed surprisingly little.

For the lower legs, data from the two studies are as follows:

Quantity	McConville et al. (1980)	UMTRI Standing	UMTRI Seated
Calf Length	407.4	401.8	
Calf Circumference	376.8	367.4	372.9
Ankle Circumference	224.3		229.5
Knee Circumference	374.1		392.2
Ankle Breadth	59.0		72.7 (61.2)
Knee Breadth	96.1		101.3
Calf Depth	120.2		117.7

These data are very similar. The knee circumference is larger for the UMTRI subjects due to flexion. The reason for the large difference in ankle breadths is unknown. UMTRI measurements include a minimum ankle breadth of 61.2.

For the feet, data from the two studies are as follows:

Quantity	McConville et al. (1980)	UMTRI Standing	UMTRI Seated
Foot Length	266.1	264.0	
Foot Breadth	104.9	95.7	
Sphyrion Height	70.7		80.0
Ankle Circumference	224.3		229.5
Arch Circumference	260.1		
Ball of Foot Circumference	257.3		

These data are fairly similar. Sphyrion height is defined to be the perpendicular distance from toeboard to sphyrion. It is believed this value is larger for the seated case because very little force is exerted on the foot in a normal seated position.

As a supplement to the study of the basic geometric properties of the body, a series of surface profile measurements was made on the original clay version of the surface form shortly before castings were made. Thin strips of paper were laid on the surface of the form to represent "tops, bottoms, and sides" of the various regions of the body. Figures 8, 9, and 10 show side, front, and back views of the clay form with strips attached. Points along these strips were digitized in three dimensions using a mechanical measurement frame. The coordinates of these surface points are included in Table 9. These points have been used in Figure 1 of this report and the full-size drawings (Blueprint Nos. MM-101, MM-102, MM-103, MM-104, and MM-105). Also, they have been used as an aid in reconstructing some of the non-standard anthropometry discussed in this section of the report.

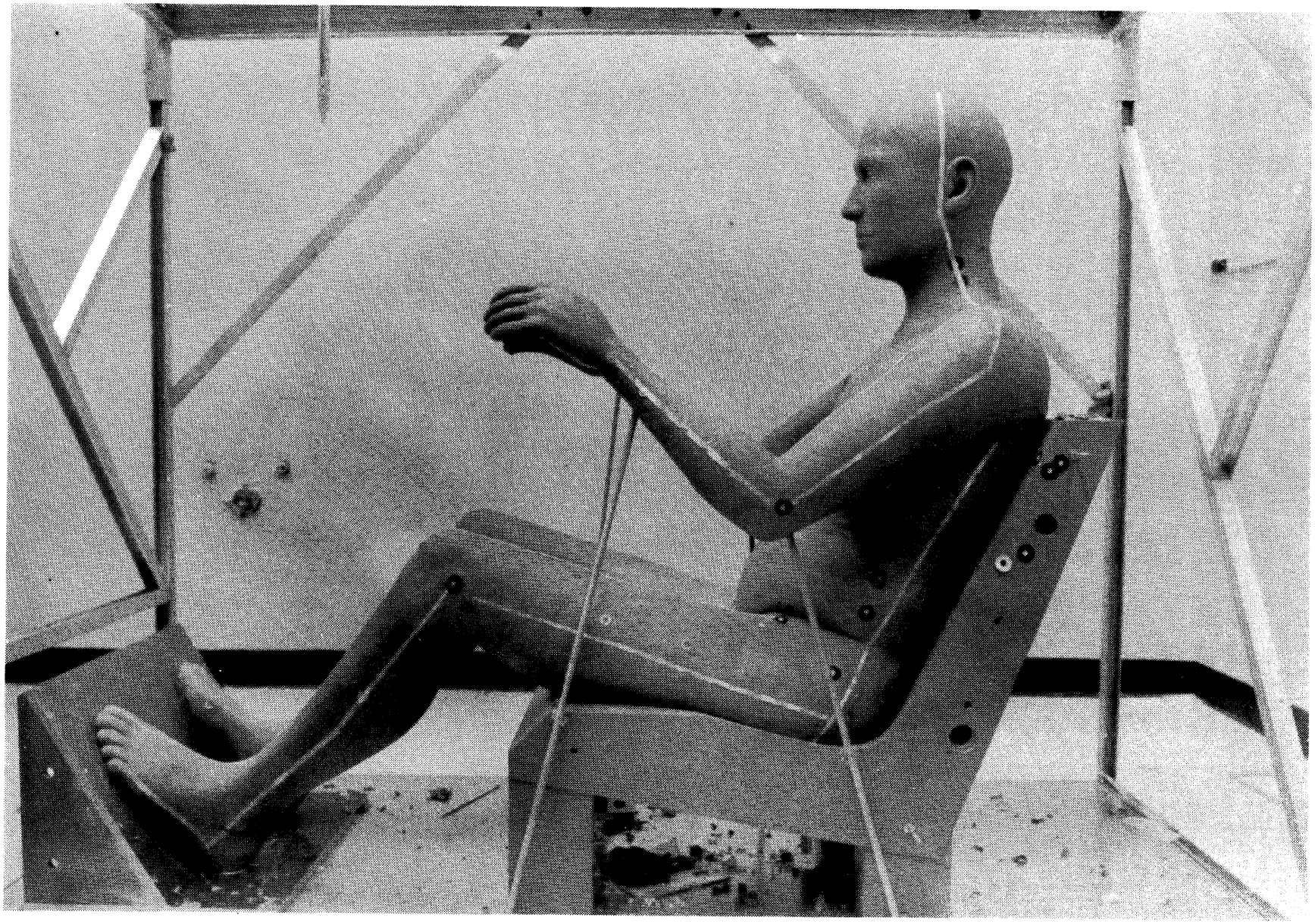

FIGURE 8. Side view of clay model with surface profile strips.

FIGURE 9. Front view of clay model with surface profile strips.

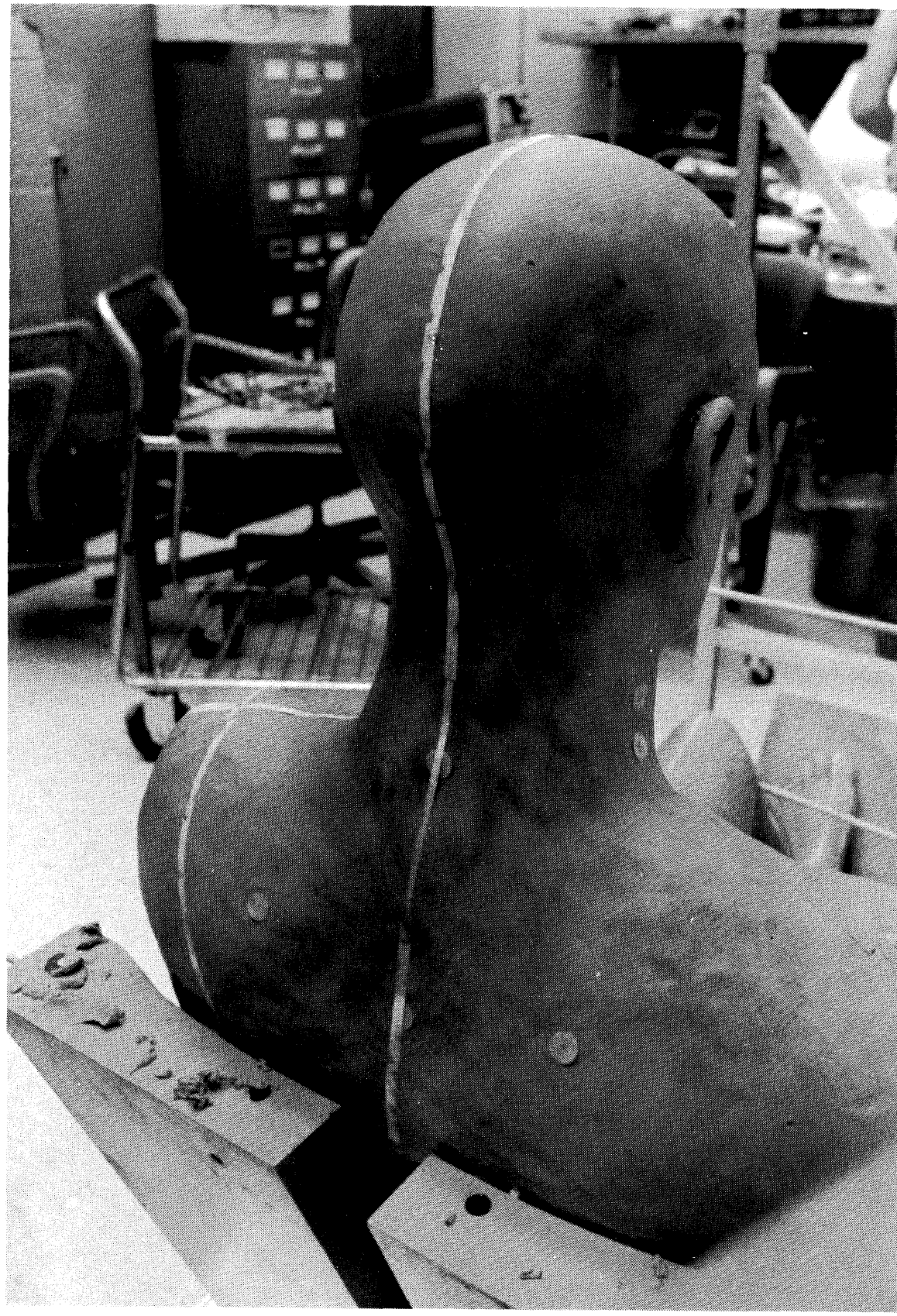

FIGURE 10. Back view of clay model with surface profile strips.

TABLE 9

COORDINATES OF SURFACE POINTS ON CLAY FORM (mm)

Surface Point	X_H	Y_H	Z_H
Body center from crotch up front of body, over head, down back to seat intersection	62	0	55
	62	0	99
	54	0	132
	31	0	170
	7	0	201
	- 31	0	240
	- 51	0	283
	- 76	0	343
	-100	0	386
	-127	0	415
	-139	0	433
	-149	0	443
	-150	0	470
	-143	0	493
	-120	0	504
	- 95	0	518
	- 93	0	535
	- 86	0	549
	- 84	0	561
	- 85	0	575
	- 65	0	589
	- 83	0	634
	- 80	0	650
	- 81	0	664
	- 88	0	693
	- 96	0	707
	-122	0	727
	-164	0	737
	-194	0	739
	-229	0	730
	-252	0	712
	-267	0	693
	-278	0	665
	-280	0	640
	-264	0	591
	-257	0	569
	-258	0	519
	-267	0	476
	-277	0	438
	-289	0	383
	-299	0	330
	-287	0	265
	-260	0	184

TABLE 9
COORDINATES OF SURFACE POINTS ON CLAY FORM (Continued)

Surface Point	X_H	Y_H	Z_H
Line from posterior scye up back, over shoulder, and down top of arm to hand	-297	112	336
	-292	131	392
	-275	141	419
	-262	146	432
	-240	150	446
	-224	156	449
	-209	161	449
	-190	168	447
	-160	176	432
	-126	184	405
	- 84	188	367
	- 27	195	326
	31	204	277
	37	205	274
	69	200	302
	110	194	328
	133	188	342
	163	175	364
	201	164	399
	219	156	417
	228	149	433
	237	141	446
	254	132	460
	274	124	468
Line from top of head to lateral point on shoulder	-185	0	735
	-182	29	730
	-178	57	711
	-175	74	679
	-174	79	642
	-175	74	588
	-182	69	552
	-192	57	524
	-204	61	491
	-208	71	473
	-213	116	456
	-215	170	447
	-213	202	431
	-206	222	407
	-196	231	378
Line from lateral point on shoulder down outside of arm to ulnar styloid process	-154	236	352
	- 97	235	313
	- 42	236	272
	33	241	223
	66	244	245
	111	232	284

TABLE 9
COORDINATES OF SURFACE POINTS ON CLAY FORM (Continued)

Surface Point	X_H	Y_H	Z_H
Line from lateral point on shoulder down outside of arm to ulnar styloid process (Continued)	152	211	321
	188	197	354
	207	191	373
	222	191	388
Line down side of torso from posterior scye to seat surface	-217	189	294
	-190	179	250
	-166	169	204
	-144	157	164
	-120	169	119
	- 98	162	81
	- 82	157	54
	- 64	182	23
	- 47	196	- 5
	- 36	198	- 22
	- 26	199	- 37
Outside of left leg from hip to little toe	- 31	200	- 21
	36	204	1
	133	204	33
	237	206	70
	322	200	97
	379	194	113
	405	188	129
	429	186	94
	469	187	45
	511	180	- 7
	553	168	- 57
	590	148	- 89
	627	131	-122
	655	122	-149
	694	122	-185
	719	129	-210
	752	149	-165
	784	171	-123
	807	177	- 98
Underside of leg from seat front to heel	311	129	- 1
	360	129	31
	403	129	57
	417	138	25
	453	134	- 45
	512	123	- 93
	566	113	-126
	617	100	-162
	650	93	-205
	667	91	-229

TABLE 9
COORDINATES OF SURFACE POINTS ON CLAY FORM (Continued)

Surface Point	X_H	Y_H	Z_H
Top of leg from thigh-abdominal junction to tips of second toe (tips of all toes included)	18	123	79
	63	125	88
	167	134	116
	244	132	140
	318	145	162
	412	151	190
	449	151	170
	478	149	127
	510	146	82
	572	139	0
	641	115	- 79
	676	106	-107
	701	102	-114
	729	103	-109
	764	108	- 89
	801	117	- 68
	840	129	- 36
	843	150	- 42
	836	164	- 59
	827	172	- 76
	814	177	- 92
Inside of leg from crotch to metatarsal/phalangeal I	190	30	16
	235	48	33
	293	64	58
	355	75	95
	395	85	134
	424	91	130
	445	89	92
	467	82	58
	490	77	22
	518	76	- 20
	579	80	- 72
	640	74	-121
	673	67	-144
	713	67	-164
	743	76	-175
	703	71	-140
	736	82	-123
	777	87	- 95
	796	88	- 84
	823	103	- 59
	840	110	- 44

TABLE 9
COORDINATES OF SURFACE POINTS ON CLAY FORM (Continued)

Surface Point	X_H	Y_H	Z_H
Inside of arm from scye to fingers	- 28	151	276
	14	160	231
	38	166	205
	80	153	237
	117	147	275
	165	142	336
	202	138	381
Line on underside of arm from level of scye to wrist	-208	191	302
	-155	194	283
	- 99	196	248
	13	197	191
	42	199	182
	94	194	211
	144	181	259
	183	175	309
	222	167	355
	240	174	378
	262	184	385
	281	191	398
	303	199	409

8.2 Volume and Mass Properties

To compute the segment volumes, the regression equations given in McConville et al. (1980) were used. The following list indicates which anthropometric variables were included for each segment:

Segment	Variables
Head	Head circumference and length
Neck	Subject weight, neck circumference and breadth
Thorax	Subject weight, chest circumference, thorax length
Abdomen	Subject weight, abdomen length, waist circumference
Pelvis	Buttock circumference, suprailiac skinfold
Upper Arms	Subject weight, biceps circumference flexed, Acromion-radiale length
Lower Arms (with Hands)	Subject weight, elbow breadth, Mid-forearm circumference
Upper Legs	Subject weight, mid-thigh circumference, stature
Lower Legs	Stature, weight
Feet	Ankle circumference, stature, sphyrion height

The predicted volumes and the sum of volumes for the whole body are given in the first column of Table 10. The values obtained from the left and right sides of the body have been averaged. These volume calculations are based on a density assumption of 1.0 g/cm^3. Using this value for density, the resulting body weight would be 176.9 pounds, an overestimate of about 4.6 percent. Because of this apparent overestimation of volume, a correction factor was developed as follows:

$$\text{Volume Correction Factor} = \frac{\text{Average Subject Mass}}{\text{Initial Prediction}} = 0.954$$

Scaled volumes and estimated masses are given in the final two columns of Table 10.

It should be noted that an overestimation of volume was expected and is a subject of continuing investigation by the McConville et al. team as indicated in their report. The correction factor is similar to their 5 percent figure. Also, it should be noted that the human body does not have a constant density within each segment. For example, if a value of less than 1.0 is used for the thorax as has been suggested by Dempster (1955a), the necessary correction can be reduced considerably.

TABLE 10

ESTIMATED SEGMENT MASS AND VOLUME

Segment	Predicted Volume (cm^3)	Scaled Volume (cm^3)	Estimated Mass (gm)
Head	4,337	4,137	4,137
Neck	1,012	965	965
Thorax	24,909	23,763	23,763
Abdomen	2,479	2,365	2,365
Pelvis	11,964	11,414	11,414
Right Upper Arm	1,854	1,769	1,769
Left Upper Arm	1,854	1,769	1,769
Right Lower Arm with Hand	2,120	2,022	2,022
Left Lower Arm with Hand	2,120	2,022	2,022
Right Upper Leg	9,029	8,614	8,614
Left Upper Leg	9,029	8,614	8,614
Right Lower Leg	3,760	3,587	3,587
Left Lower Leg	3,760	3,587	3,587
Right Foot	1,028	981	981
Left Foot	1,028	981	981
TOTAL	80,254	76,562	76,562

Using his value of 0.92, thorax mass predicted from the regression equation is 22916 gm. This reduces thorax weight (predicted using density=1.0 gm/cm^3) from 54.9 pounds to 50.5 pounds. Using this adjusted thorax value in computing total body weight, the correction factor is reduced to 2.1 percent. Clearly a considerable amount of work is required before final mass and inertial data can be recommended with confidence.

8.3 Centers of Gravity in Hip Point and Segment Coordinate Systems

McConville et al. (1980) give data on center of volume for the various segments of the body. The assumption is made for the current project that center of mass and center of volume are coincident. It is known that this assumption is not completely correct because of density variations within segments. Clauser et al. (1969) note that mid-volume of limb segments are proximal to centers of mass. The differences,

however, are small and believed to be insignificant in comparison with other possible errors. The greatest of these is the mobility of soft tissues with respect to the bony skeleton as the body moves either voluntarily or especially under impact loading. For the current static case of seated posture, and for applications where the assumption of an articulated linkage of rigid masses is valid, the forestated assumption is believed to be adequate. However, if these data are to be used for dynamic applications where there is loose coupling between soft tissue and bony skeleton, the assumption should be rejected and substitute data gathered. To the knowledge of the present author, there are no substantive published data available to address this issue for automotive applications.

Table 11 gives the location of estimated centers of gravity with respect to the whole-body coordinate system. These were derived from the data in Table 12, which locate the points in segment coordinates through the use of the transformations presented in Section 7 of this report. Average values are shown for the left and right sides of the body.

It should be noted that the head center-of-gravity is given with respect to the UMTRI definition of the origin. The placement is thus in front of, and above, the origin as discussed in detail in Section 7.1.

In the case of the neck, the center of mass is a few millimeters in front of a line connecting the estimated head/neck and neck/thorax joints (see Figure 1 and Section 9 for graphics and details of joint locations).

The thorax center-of-gravity lies approximately 40 mm in front of and 20 mm below the reconstructed T8/T9 joint centers. This is a somewhat larger value than that reported by Chandler and Young (1981) in their recent link man analysis. It is believed that the forward migration of soft tissue during the process of sitting down may well account for the shift.

The center of gravity of the abdomen mass is in the center of the mass as projected in the $X_H Z_H$ plane shown in Figure 1. It is located about 2 cm in front of the spinal linkage. If, at a later time,

TABLE 11

LOCATION OF ESTIMATED SEGMENT CENTERS OF GRAVITY WITH RESPECT TO WHOLE-BODY COORDINATE SYSTEM

Segment	X_H (mm)	Y_H (mm)	Z_H (mm)
Head	-179	0	646
Neck	-195	0	515
Thorax	-177	0	267
Abdomen	- 85	0	110
Pelvis	- 74	0	17
Upper Arms	- 80	±191*	319
Lower Arms with Hands	149	±174	320
Upper Legs	200	±131	64
Lower Legs	504	±125	- 5
Feet	763	±110	-164

*The positive sign on Y_H refers to the left side of the body.

TABLE 12

LOCATION OF ESTIMATED SEGMENT CENTERS OF GRAVITY WITH RESPECT TO THE INDIVIDUAL SEGMENT COORDINATE SYSTEMS*

Segment	X_A (mm)	Y_A (mm)	Z_A (mm)
Head	8.4	0.	31.
Neck	57.2	0.	49.8
Thorax	58.	0.	190.
Abdomen	- 4.	0.	- 24.2
Pelvis	-81.8	0.	10.7
Upper Arm (R)	16.5	30.	-172.
Upper Arm (L)	16.5	-30.	-172.
Lower Arm with Hand (R)	-10.	35.	-166.
Lower Arm with Hand (L)	-10.	-35.	-166.
Upper Leg (R)	6.	66.	-200.
Upper Leg (L)	6.	-66.	-200.
Lower Leg (R)	-11.9	-57.	-149.
Lower Leg (L)	-11.9	57.	-149.
Foot (R)	-76.9	- 0.6	- 6.2
Foot (L)	-76.9	0.6	- 6.2

*Recall that there is a different (X_A, Y_A, Z_A) system for each segment.

the abdomen segmentation plane proposed earlier in this report is used, the center of gravity will be shifted even further toward the front of the body. This mass element is believed to be very mobile and loosely coupled to the remainder of the body linkage system.

For the pelvis, the center of gravity is nearly on the line of the spinal column projected into the pelvic region. It lies approximately 2 cm below the L5/S1 joint and 75 mm behind and 17 mm above the hip pivot point. It is not surprising that this mass is far toward the back in that the soft tissue surrounding the head of the femur has been attached to the upper leg segments.

The values for the upper arms, lower arms including hands, upper legs, lower legs, and feet are averaged for the right and left sides of the body. The centers of gravity for the lower arms and upper legs lie virtually on the line connecting the proximal and distal joint centers. The center of gravity of the upper arm lies above the similar line while for the lower leg the center of gravity is below it. This probably reflects the location of major muscle masses (biceps brachii and triceps surae).

8.4 Inertial Properties and Principal Axes

To compute the segment principal moments of inertia, the regression equations given in McConville et al. (1980) were used. These equations predict each of the three principal moments of inertia (I_x, I_y, I_z) for each segment as a linear function of anthropometric variables. Table 13 lists the anthropometric variables used in computing each quantity. The predicted segment inertial properties are given in the first three columns of Table 14. Values from the left and right sides of the body have been averaged. The principal axes (X_p, Y_p, Z_p) for each segment have their origin at the center of gravity (assumed to be coincident with the center of volume). The orientation of these axes is dependent on the geometric form of each individual segment and represents yet another group of coordinate systems.

It appears that the magnitudes of both volume and inertial properties are overestimated by the McConville et al. formulae. In a simplistic sense, the overall composition of a moment of inertia is the

TABLE 13

ANTHROPOMETRIC VARIABLES USED IN PRINCIPAL MOMENT OF INERTIA REGRESSION EQUATIONS

Segment	Moment	Anthropometric Variables
Head	I_X	Head circumference, head breadth
	I_Y	Head circumference
	I_Z	Head circumference, head length
Neck	I_X	Neck breadth, neck length
	I_Y	Weight, neck circumference, neck breadth
	I_Z	Weight, neck circumference, neck breadth
Thorax	I_X	Weight, thorax length, chest breadth
	I_Y	Weight, stature, thorax length
	I_Z	Weight, chest circumference, thorax length
Abdomen	I_X	Abdomen length, waist circumference, suprailiac skinfold
	I_Y	10th rib circumference, abdomen length, suprailiac skinfold
	I_Z	Waist circumference, abdomen length, suprailiac skinfold
Pelvis	I_X	Buttock circumference, suprailiac skinfold, buttock depth
	I_Y	Buttock depth
	I_Z	Buttock depth, weight, suprailiac skinfold
Upper Arms	I_X	Weight, acromion-radiale length, biceps circumference (flexed)
	I_Y	Weight, triceps skinfold, axilla arm depth
	I_Z	Biceps circumference (flexed), axilla arm circumference, acromion-radiale length
Lower Arms (with hands)	I_X	Forearm-hand length, wrist and hand circumferences
	I_Y	Forearm-hand length, wrist and hand circumferences
	I_Z	Elbow and mid-forearm circumferences, weight
Upper Legs	I_X	Weight, mid-thigh circumference, thigh length
	I_Y	Stature, mid-thigh circumference, thigh length
	I_Z	Weight, mid-thigh and upper-thigh circumferences
Lower Legs	I_X	Stature, calf depth, ankle circumference
	I_Y	Stature, calf depth, ankle circumference
	I_Z	Weight, calf length, calf circumference
Feet	I_X	Ankle circumference, sphyrion height, stature
	I_Y	Foot length, sphyrion height, ankle circumference
	I_Z	Foot length, ankle circumference, sphyrion height

TABLE 14

ESTIMATED SEGMENT PINCIPAL MOMENTS OF INERTIA

Segment	Predicted (gm cm^2)			Scaled (gm cm^2)		
	I_X	I_Y	I_Z	I_X	I_Y	I_Z
Head	206,678	228,634	149,176	200,271	221,546	144,552
Neck	15,271	19,054	23,643	14,798	18,463	22,910
Thorax	4,712,487	3,325,653	3,112,360	4,566,400	3,222,558	3,015,877
Abdomen	172,973	109,969	262,991	167,611	106,560	254,838
Pelvis	1,048,233	972,524	1,222,598	1,015,738	942,376	1,184,697
Up. Arm (L)	116,065	126,446	23,854	112,467	122,526	23,115
Up. Arm (R)	116,065	126,446	23,854	112,467	122,526	23,115
Low. Arm & Hand (L)	320,711	319,145	20,793	310,769	309,252	20,148
Low. Arm & Hand (R)	320,711	319,145	20,793	310,769	309,252	20,148
Up. Leg (L)	1,270,278	1,343,179	378,863	1,230,899	1,301,540	367,118
Up. Leg (R)	1,270,278	1,343,179	378,863	1,230,899	1,301,540	367,118
Low. Leg (L)	537,045	545,245	62,629	520,397	528,342	60,688
Low. Leg (R)	537,045	545,245	62,629	520,397	528,342	60,688
Foot (L)	9,007	44,341	45,544	8,728	42,966	44,132
Foot (R)	9,007	44,341	45,544	8,728	42,966	44,132

summation of infinitesimal mass elements times the square of their distances from an axis about which the moment is computed. Therefore, if the volume is reduced, the representative distances from the axis are also reduced. Volume can be visualized as a third order function of distances while inertial moments are second order. A scale factor has been developed based on the 0.954 reduction factor for volume used in Section 8.2 as follows:

$$\text{Volume (UMTRI)} = 0.954V \sim (0.9844\ell^3)$$

$$\text{Scale Factor} = (0.9844)^2 = 0.969$$

This factor has been used in the computation of scaled segment inertial properties given in the last three columns of Table 14. In that McConville et al. show some evidence that their predicted inertial properties have larger magnitudes than those proposed by other investigators, it is felt that a small correction factor is justified. The one proposed may be too conservative as the mass on the periphery of an object has a greater effect on moment of inertia than mass near the center of gravity.

The principal axes of inertia for each segment have been computed by McConville et al. with respect to the respective segment anatomical coordinate system. For the present application, it has been necessary to alter the transformation matrices slightly to reflect body symmetry. In the case of body segments such as head, neck, thorax, abdomen, and pelvis, this meant setting small direction angles between the Y-principal axis and the Y-segment axis to zero and adjusting the remainder of the transformation slightly to maintain orthogonality. A typical example is the head. The transformations given by McConville et al. in degrees are:

	X_A	Y_A	Z_A
X_P	36.13	86.95	54.04
Y_P	93.75	3.75	90.02
Z_P	125.88	92.19	35.96

For symmetry this has been simplified to:

	X_A	Y_A	Z_A
X_P	36	90	54
Y_P	90	0	90
Z_P	125	90	36

The quantities (X_A, Y_A, Z_A) refer to anatomical coordinates while (X_P, Y_P, Z_P) refer to principal axes.

In the case of body regions, such as upper and lower arms and legs as well as feet, it was necessary to develop an average set of axes for the two sides, then to make it symmetric. A typical case of this is for the feet. The transformations for the left and right feet were given as:

Right Foot

	X_A	Y_A	Z_A
X_P	9.85	85.95	81.04
Y_P	95.18	8.76	82.95
Z_P	98.35	97.75	11.14

Left Foot

	X_A	Y_A	Z_A
X_P	8.97	92.17	81.30
Y_P	87.21	4.83	93.94
Z_P	98.52	85.69	9.56

They have been simplified, averaged, and made symmetric yielding:

Right Foot

	X_A	Y_A	Z_A
X_P	10	86	81
Y_P	94	7	85
Z_P	99	95	10

Left Foot

	X_A	Y_A	Z_A
X_P	10	94	81
Y_P	86	7	95
Z_P	99	85	10

Problems with the McConville et al. data were identified for the right thigh and left forearm (with hand). These were confirmed (Kaleps 1982) as incorrect signs in coordinate system definitions. In cases where the symmetry appeared to be marginal between the two sides of the body, it was verified that the transformation matrix degenerates when two of the moments of inertia become the same.

The final results are given in Tables 15 through 18. Tables 15 and 16 give the principal axes of inertia with respect to anatomical axes expressed both in degrees and as cosines. Tables 17 and 18 give the principal axes with respect to the hip point axis system.

TABLE 15

PRINCIPAL AXES OF INERTIA WITH RESPECT TO ANATOMICAL AXES
(Cosine Matrix Expressed in Degrees)

Segment		X_A	Y_A	Z_A
Head	X_P	36.	90.	54.
	Y_P	90.	0.	90.
	Z_P	126.	90.	36.
Neck	X_P	11.	90.	79.
	Y_P	90.	0.	90.
	Z_P	101.	90.	11.
Thorax	X_P	14.5	90.	75.5
	Y_P	90.	0.	90.
	Z_P	104.5	90.	14.5
Abdomen	X_P	2.6	90.	92.2
	Y_P	90.	0.	90.
	Z_P	87.8	90.	2.6
Pelvis	X_P	8.4	90.	81.6
	Y_P	90.	0.	90.
	Z_P	98.4	90.	8.4
Upper Arm (L)	X_P	33.6	56.6	91.1
	Y_P	123.4	34.3	83.
	Z_P	90.	96.1	7.
Upper Arm (R)	X_P	33.6	123.4	91.1
	Y_P	56.6	34.3	96.1
	Z_P	90.	83.	7.
Lower Arm with Hand (L)	X_P	19.5	70.5	90.
	Y_P	109.5	19.5	90.
	Z_P	90.	90.	1.
Lower Arm with Hand (R)	X_P	19.5	109.5	90.
	Y_P	70.5	19.5	90.
	Z_P	90.	90.	1.
Upper Leg (L)	X_P	9.8	80.2	89.8
	Y_P	99.8	9.8	90.9
	Z_P	90.1	89.1	1.1
Upper Leg (R)	X_P	9.8	99.8	89.8
	Y_P	80.2	9.8	90.9
	Z_P	90.1	89.1	1.1

TABLE 15
PRINCIPAL AXES OF INERTIA WITH RESPECT TO ANATOMICAL AXES
(Cosine Matrix Expressed in Degrees, Continued)

Segment		X_A	Y_A	Z_A
Lower Leg (L)	X_P	24.	114.	90.
	Y_P	66.	24.	92.
	Z_P	90.	88.	1.
Lower Leg (R)	X_P	24.	66.	90.
	Y_P	114.	24.	88.
	Z_P	90.	92.	1.
Foot (L)	X_P	10.	94.	81.
	Y_P	86.	7.	95.
	Z_P	99.	85.	10.
Foot (R)	X_P	10.	86.	81.
	Y_P	94.	7.	85.
	Z_P	99.	95.	10.

TABLE 16

PRINCIPAL AXES OF INERTIA WITH RESPECT TO ANATOMICAL AXES
(Cosine Matrix)

Segment		X_A	Y_A	Z_A
Head	X_P	0.809	0.	0.588
	Y_P	0.	1.	0.
	Z_P	-0.588	0.	0.809
Neck	X_P	0.981	0.	0.192
	Y_P	0.	1.	0.
	Z_P	-0.192	0.	0.981
Thorax	X_P	0.968	0.	0.250
	Y_P	0.	1.	0.
	Z_P	-0.250	0.	0.968
Abdomen	X_P	0.999	0.	-0.038
	Y_P	0.	1.	0.
	Z_P	0.038	0.	0.999
Pelvis	X_P	0.989	0.	0.146
	Y_P	0.	1.	0.
	Z_P	-0.146	0.	0.989
Upper Arm (L)	X_P	0.829	0.545	-0.0175
	Y_P	-0.559	0.829	-0.104
	Z_P	0.	0.122	0.992
Upper Arm (R)	X_P	0.829	-0.559	-0.0175
	Y_P	0.545	0.829	0.122
	Z_P	0.	-0.104	0.992
Lower Arm with Hand (L)	X_P	0.943	0.334	0.
	Y_P	-0.334	0.943	0.
	Z_P	0.	0.	1.
Lower Arm with Hand (R)	X_P	0.943	-0.334	0.
	Y_P	0.334	0.943	0.
	Z_P	0.	0.	1.
Upper Leg (L)	X_P	0.985	0.170	0.00349
	Y_P	-0.170	0.985	-0.0157
	Z_P	-0.00175	0.0157	1.
Upper Leg (R)	X_P	0.985	-0.170	0.00349
	Y_P	0.170	0.985	-0.0157
	Z_P	-0.00175	0.0157	1.

TABLE 16
PRINCIPAL AXES OF INERTIA WITH RESPECT TO ANATOMICAL AXES
(Cosine Matrix, Continued)

Segment		X_A	Y_A	Z_A
Lower Leg (L)	X_P	0.913	-0.407	0.000
	Y_P	0.407	0.913	-0.0349
	Z_P	0.	0.0349	1.
Lower Leg (R)	X_P	0.913	0.407	0.
	Y_P	-0.407	0.913	0.0349
	Z_P	0.	-0.0349	1.
Foot (L)	X_P	0.985	-0.0698	0.156
	Y_P	0.0698	0.992	-0.0872
	Z_P	-0.156	0.0872	0.985
Foot (R)	X_P	0.985	0.0698	0.156
	Y_P	-0.0698	0.992	0.0872
	Z_P	-0.156	-0.0872	0.985

TABLE 17

PRINCIPAL AXES OF INERTIA WITH RESPECT TO HIP POINT AXIS SYSTEM
(Cosine Matrix Expressed in Degrees)

Segment		X_H	Y_H	Z_H
Head	X_P	39.8	90.	50.1
	Y_P	90.	0.	90.
	Z_P	129.9	90.	39.8
Neck	X_P	9.9	90.	99.7
	Y_P	90.	0.	90.
	Z_P	80.3	90.	9.9
Thorax	X_P	22.3	0.	67.7
	Y_P	90.	1.	90.
	Z_P	112.3	0.	22.3
Abdomen	X_P	26.	90.	64.1
	Y_P	90.	0.	90.
	Z_P	115.9	90.	26.
Pelvis	X_P	69.4	90.	20.6
	Y_P	90.	0.	90.
	Z_P	159.4	90.	69.4
Upper Arm (L)	X_P	56.	72.	40.
	Y_P	106.	20.	100.
	Z_P	142.	97.	53.
Upper Arm (R)	X_P	56.	108.	40.
	Y_P	74.	20.	80.
	Z_P	142.	83.	53.
Lower Arm with Hand (L)	X_P	177.	52.	50.
	Y_P	57.	40.	109.
	Z_P	134.	78.	134.
Lower Arm with Hand (R)	X_P	117.	128.	50.
	Y_P	123.	40.	71.
	Z_P	134.	102.	134.
Upper Leg (L)	X_P	110.	74.	26.
	Y_P	83.	16.	104.
	Z_P	159.	89.	111.
Upper Leg (R)	X_P	110.	106.	26.
	Y_P	97.	16.	76.
	Z_P	159.	91.	111.

TABLE 17
PRINCIPAL AXES OF INERTIA WITH RESPECT TO HIP POINT AXIS SYSTEM
(Cosine Matrix Expressed in Degrees, Continued)

Segment		X_H	Y_H	Z_H
Lower Leg (L)	X_P	43.	92.	47.
	Y_P	85.	6.	93.
	Z_P	134.	84.	44.
Lower Leg (R)	X_P	43.	88.	47.
	Y_P	95.	6.	87.
	Z_P	134.	96.	44.
Foot (L)	X_P	69.	82.	23.
	Y_P	84.	14.	102.
	Z_P	158.	80.	71.
Foot (R)	X_P	69.	98.	23.
	Y_P	96.	14.	78.
	Z_P	158.	100.	71.

TABLE 18

PRINCIPAL AXES OF INERTIA WITH RESPECT TO HIP POINT AXIS SYSTEM
(Cosine Matrix)

Segment		X_H	Y_H	Z_H
Head	X_P	0.768	0.	0.641
	Y_P	0.	1.	0.
	Z_P	-0.641	0.	0.768
Neck	X_P	0.985	0.	-0.169
	Y_P	0.	1.	0.
	Z_P	0.169	0.	0.985
Thorax	X_P	0.925	0.	0.379
	Y_P	0.	1.	0.
	Z_P	-0.379	0.	0.925
Abdomen	X_P	0.899	0.	0.437
	Y_P	0.	1.	0.
	Z_P	-0.437	0.	0.899
Pelvis	X_P	0.352	0.	0.936
	Y_P	0.	1.	0.
	Z_P	-0.936	0.	0.352
Upper Arm (L)	X_P	0.56	0.3	0.77
	Y_P	-0.28	0.94	-0.17
	Z_P	-0.78	-0.12	0.60
Upper Arm (R)	X_P	0.56	-0.30	0.77
	Y_P	0.28	0.94	0.17
	Z_P	-0.78	0.12	0.60
Lower Arm with Hand (L)	X_P	-0.461	0.61	0.644
	Y_P	0.551	0.767	-0.332
	Z_P	-0.697	0.201	-0.689
Lower Arm with Hand (R)	X_P	-0.461	-0.61	0.644
	Y_P	-0.551	0.767	0.332
	Z_P	-0.697	-0.201	-0.689
Upper Leg (L)	X_P	-0.342	0.275	0.898
	Y_P	0.130	0.96	-0.245
	Z_P	-0.931	0.0169	-0.364
Upper Leg (R)	X_P	-0.342	-0.275	0.898
	Y_P	-0.130	0.960	0.245
	Z_P	-0.931	-0.0169	-0.364

TABLE 18
PRINCIPAL AXES OF INERTIA WITH RESPECT TO HIP POINT AXIS SYSTEM
(Cosine Matrix, Continued)

Segment		X_H	Y_H	Z_H
Lower Leg (L)	X_P	0.727	-0.026	0.685
	Y_P	0.092	0.995	-0.059
	Z_P	-0.691	0.103	0.716
Lower Leg (R)	X_P	0.727	0.026	0.685
	Y_P	-0.092	0.995	0.059
	Z_P	-0.691	-0.103	0.716
Foot (L)	X_P	0.359	0.147	0.922
	Y_P	0.11	0.969	-0.214
	Z_P	-0.93	0.168	0.328
Foot (R)	X_P	0.359	-0.147	0.922
	Y_P	-0.11	0.969	0.214
	Z_P	-0.93	-0.168	0.328

9.0 A MODEL FOR THE LOCATION OF JOINT CENTERS

9.1 Introduction

In order to quantify motions of one segment with respect to its neighbors in a linkage, it is necessary to define the connections between the elements in the linkage. Connections between elements of the bony skeleton are called articulations. If the position of the articulation coincides with a point about which rotations between neighboring bony segments can occur, it is called a center of rotation or joint center.

Joints in the human body most often exhibit more than one degree-of-freedom in describing the motion of one body segment with respect to its neighbors. Some, such as the knee and elbow, can probably be modeled as pins connecting the upper and lower arms and legs. However, it is known that the motions at these joints are more complex and involve a small amount of migration of the joint location within each of the neighboring segments as the body moves (Dempster (1955a). Others, such as the hip, ankle, and glenohumeral joints, are more like ball connections between the two segments.

The shoulder girdle is even more complex in that it is composed of three articulations: the glenohumeral, sternoclavicular, and acromioclavicular articulations. The glenohumeral articulation consists of the humeral head rotating on the glenoid fossa. As there is very little movement of the center of the humeral head with respect to the scapula in normal motion, this articulation can properly be called the glenohumeral joint. The sternoclavicular articulation has many properties of a ball joint while the acromioclavicular articulation combines with the conoid and trapezoid ligaments to form the claviscapular joint system which has been discussed by Dempster (1965). These joints are supplemented by a movable shoulder girdle mass, separate from the thorax, which rides with the scapula. The three joints, combined with the clavicle and scapula mass links, define the mobility of the arm with respect to the torso.

The vertebral column is actually a collection of seven cervical, twelve thoracic, and five lumbar vertebrae. In each articulation between the vertebrae there is the possibility of limited rotation, shear, and stretching. Two concepts have been used in the construction of cervical spines for crash test dummies such as the Hybrid III (Foster et al. 1977) and crash victim computer codes such as the MVMA 2D model (Bowman et al. 1979) and the various versions of the Calspan CVS. In the case of the dummy, the cervical spine is a deformable element connecting head to torso. The model lumps the rotational properties into head/neck and neck/thorax interface joints and uses an extensible neck link between the joints. Both concepts are simplifications of the actual vertebral structure which ignore coupling between the three possible rotational modes at the various articulations (flexion, lateral flexion, and rotation) as has been discussed by Bowman and Robbins (1972), as well as Schneider et al. (1975). This coupling is believed to exist for all lumped joint models of the vertebral column.

The thoracic vertebrae are usually assumed to be immobile with respect to each other in similar dummy and modeling applications. Studies such as the torso link mobility study by Snyder et al. (1972) and the spinal mobility study by Cheng et al. (1979) contradict each other as to the need for upgrading this model. The torso link study, which is a reach study and does not involve dynamic loading, identifies substantial mobility throughout the spine from neck to pelvis. The Wayne State study (Cheng et al. 1979) has gone so far as to suggest a rigid link from the C7/T1 to the lumbar sacral joint for use in a frontal impact dummy. It is clear that considerable work and discussion must take place before the definitive selection of the appropriate number of spinal joints and the linkage between them is resolved.

The lumbar spine is usually considered as a flexible element in dummy hardware. Alternatively, the mobility is concentrated at two joints representing connections to the pelvis and thorax. Data are very limited and incomplete, especially for non-frontal dynamic mobility, regarding both location and compliance for this joint model.

Joint center models for the seated occupant are derived from several sources and presented in the following three subsections. These

cover successively the vertebral column, the shoulder and arm, and finally, the hip, knee, and ankle. A summary of the results is given in Tables 19 and 20.

TABLE 19

LOCATION OF JOINT CENTERS IN WHOLE-BODY COORDINATES

Joint	X_H (mm)	Y_H (mm)	Z_H (mm)
Head/Neck	-196	0	588
C7/T1	-193	0	469
T4/T5	-220	0	397
T8/T9	-215	0	287
T12/L1	-177	0	165
L2/L3	-142	0	115
L5/S1	- 89	0	39
Sternoclavicular	-145	± 20	433
Claviscapular	-230	±168	427
Glenohumeral	-186	±173	393
Elbow	36	±208	201
Wrist	228	±158	393
Hip	0	± 82	0
Knee	406	±138	136
Ankle	684	± 94	-169

TABLE 20

LOCATION OF JOINT CENTERS IN SEGMENT COORDINATES

Joint	Segment	Coordinates (mm)		
		X_A	Y_A	Z_A
Head/Neck	Head	- 13	0	- 25
Head/Neck	Neck	30	0	117
C7/T1	Neck	75	0	7
C7/T1	Thorax	70	0	392
T4/T5	Thorax	32	0	338
T8/T9	Thorax	25	0	220
T12/L1	Thorax	47	0	105
L2/L3	Thorax	85	0	38
L2/L3	Abdomen	- 39	0	6
L5/S1	Abdomen	- 40	0	- 87
L5/S1	Pelvis	- 67	0	29
Sternoclavicular (L)	Thorax	106	43	347
Sternoclavicular (R)	Thorax	106	- 43	347
Claviscapular (L)	Thorax	21	168	354
Claviscapular (R)	Thorax	21	-168	354
Glenohumeral (L)	Thorax	60	173	314
Glenohumeral (R)	Thorax	60	-173	314
Glenohumeral (L)	Upper Arm (L)	12	- 33	- 42
Glenohumeral (R)	Upper Arm (R)	12	33	- 42
Elbow (L)	Upper Arm (L)	- 6	- 39	-337
Elbow (R)	Upper Arm (R)	- 6	39	-337
Elbow (L)	Lower Arm (L)	- 11	- 35	5
Elbow (R)	Lower Arm (R)	- 11	35	5
Wrist (L)	Lower Arm (L)	- 7	- 30	-271
Wrist (R)	Lower Arm (R)	- 7	30	-271
Hip (L)	Pelvis	- 61	82	- 62
Hip (R)	Pelvis	- 61	- 82	- 62
Hip (L)	Upper Leg (L)	13	-123	7
Hip (R)	Upper Leg (R)	13	123	7
Knee (L)	Upper Leg (L)	0	- 51	-418
Knee (R)	Upper Leg (R)	0	51	-418
Knee (L)	Lower Leg (L)	12	48	22
Knee (R)	Lower Leg (R)	12	- 48	22
Ankle (L)	Lower Leg (L)	0	37	-393
Ankle (R)	Lower Leg (R)	0	- 37	-393
Ankle (L)	Foot (L)	-124	- 14	58
Ankle (R)	Foot (R)	-124	14	58

9.2 Joint Center Model for the Vertebral Column

A stated goal of the project was to obtain the spatial location for a seated person of the following vertebral joint centers:

Head/Neck Interface	T12/L1
C7/T1	L2/L3
T4/T5	L5/S1
T8/T9	

This is a considerable reduction in the possible degrees of freedom when all elements of the vertebral column are taken into account, particularly with respect to the neck. However, it does break the spine in sufficiently small segments to fairly accurately define its overall position in space with respect to the remaining skeletal elements of the body such as the head, shoulder girdle, rib cage, and pelvis. Also, there is a reasonable data base available which can be adapted to this task.

The most commonly accepted location for a joint at the head/neck interface is at the occipital condyles. Mertz and Patrick (1971) and Ewing and Thomas (1973) have used this point for presentation of neck torque data. Its location has been given in anatomical coordinates constructed from targets on the superior edge of each auditory meatus and at the infraorbital notches (Ewing and Thomas 1972). Although tragion, as used in the present study, and external auditory meatus are different anatomical entities, and there is bound to be some variation between individuals in shape and exact location of tragus, there probably is no more variation than in taking the measurement itself. So, it will be assumed that the coordinate system of Ewing and Thomas (1972) is coincident with that of the present project. The average distance from origin to occipital condyle point is thus assumed to be X_A=-11, Z_A=-26, which are averages from Table 3 of the Ewing and Thomas report (1973). In the UMTRI coordinate system based on the hip point, this places the head/neck joint center at:

$$X_H=-196,\ Y_H=0,\ Z_H=588.$$

The location is graphically displayed in Figure 1.

The Snyder et al. report (1972), dealing with the link system of the human torso, provides the only known source of data which relates

external spinal landmarks to vertebral interspaces. As such, it has been used to construct the spinal linkage from the C7/T1 to the lumbar/sacral interface. The seated posture used in the torso link study was most often more erect than that assumed in the automobile seated posture. However, the position of the arm in the current study was about the mid-range for most of those assumed by subjects in the torso link study.

Figure 11 shows the geometric construction of the C7/T1 interface using torso link data. Cervical vector prediction equations were used. These required the availability of C7 and nasion surface markers. The angle of a vector from C7 to glabella with the vertical was entered into the appropriate regression equation to yield the distance from the C7 surface marker to the C7/T1 interspace as well as the angle made by the vector connecting C7 to the C7/T1 interspace (74.7 degrees). The use of glabella instead of nasion resulted in a difference of about one millimeter in the location of the joint center.

Similarly, thoracic vector prediction equations were used in estimating the T4/T5, T8/T9, and T12/L1 interfaces. These required the availability of T4 and T12 surface markers. The angle between a line connecting these two points and a vertical line serves as the reference angle for use in the regression equations. These equations are then used to predict the following:

- Distance from T4 to T4/T5 interspace
- Vector direction from T4 to T4/T5 interspace
- Distance from T8 to T8/T9 interspace
- Vector Direction from T8 to T8/T9 interspace
- Distance from T12 to T12/L1 interspace
- Vector direction from T12 to T12/L1 interspace

The reconstruction is shown in Figure 12.

Even though the regression equations in the torso link study had no obvious data available for defining a reference angle in the lumbar region of the back (interior landmarks were required) several techniques using the L2 and L5 surface targets were attempted. The techniques involved backwards solution of the regression equations for the interior reference angle using surface target coordinates to develop the input. The solution of each equation led to a different value for the interior

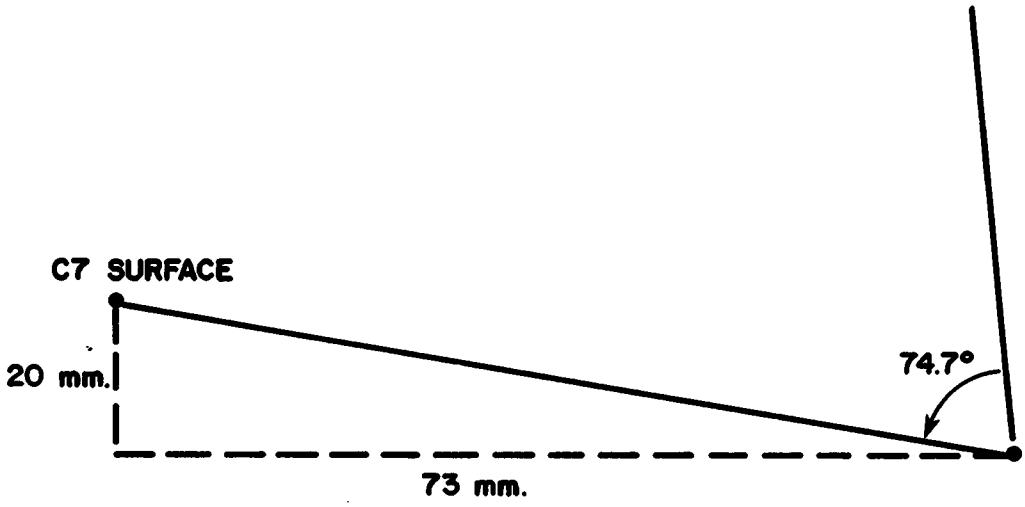

FIGURE 11. Construction of C7/T1 joint.

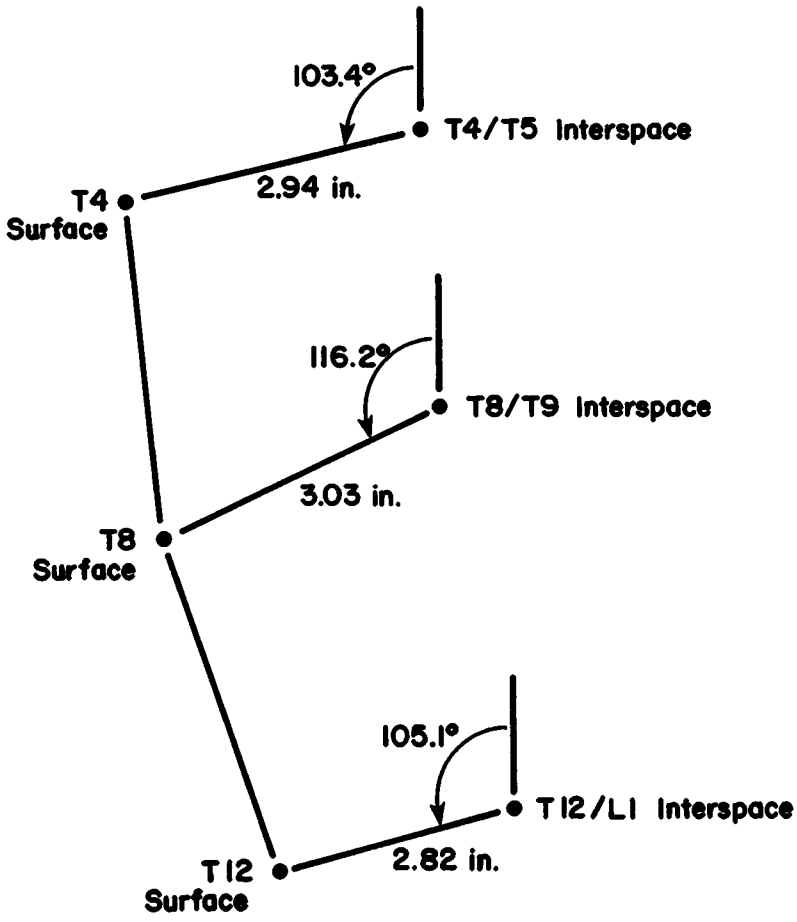

FIGURE 12. Construction of thoracic joints.

angle. When these values were used for frontwards solution and prediction, a similar variety of interspace locations were predicted. These estimations for the L2/L3 and L5/S1 interspace locations were clustered in a circle with a radius of about 5 mm for the L5/S1 interface and about 7 mm for the L2/L3 interface. It was also noted that the lateral point on the first sacral vertebral body, determined from the Reynolds et al. (1981) data and discussed in Section 3, was within the circle for L5/S1 predictions. Because of this, a simpler procedure has been adopted which yields interface points within these circles. As a first step, the lateral point on the first sacral vertebral body was chosen to represent the connection of the vertebral column to the pelvis (or L5/S1 joint). As a second step, a straight line was constructed from this point to the predicted T12/L1 interface. The assumption was then made that the thicknesses of the lumbar vertebral bodies are similar. This led to the approximation that the L2/L3 interface is 60 percent of the way from the pelvis to the T12/L1 interface. The point defined by this construction lies within the circle of estimates discussed above. The results of this reconstruction are shown in Figure 13.

9.3 Joint Centers in the Shoulder and Arm

The shoulder girdle is the structure which connects the arms to the remainder of the bony skeleton. This structure, often represented by a simple ball joint in crash test dummies, actually consists of three independent joints and two bony links. The joints are the:

1. Sternoclavicular joint where the clavicle meets the sternum
2. Claviscapular joint which models the complex connection of the scapula to the clavicle (Dempster 1965)
3. Glenohumeral joint where the humerus interacts with the scapula at the glenoid fossa

The bony links can be modeled as:

1. The clavicle from the sternoclavicular to the claviscapular joint
2. The scapula from the claviscapular to the glenohumeral joint

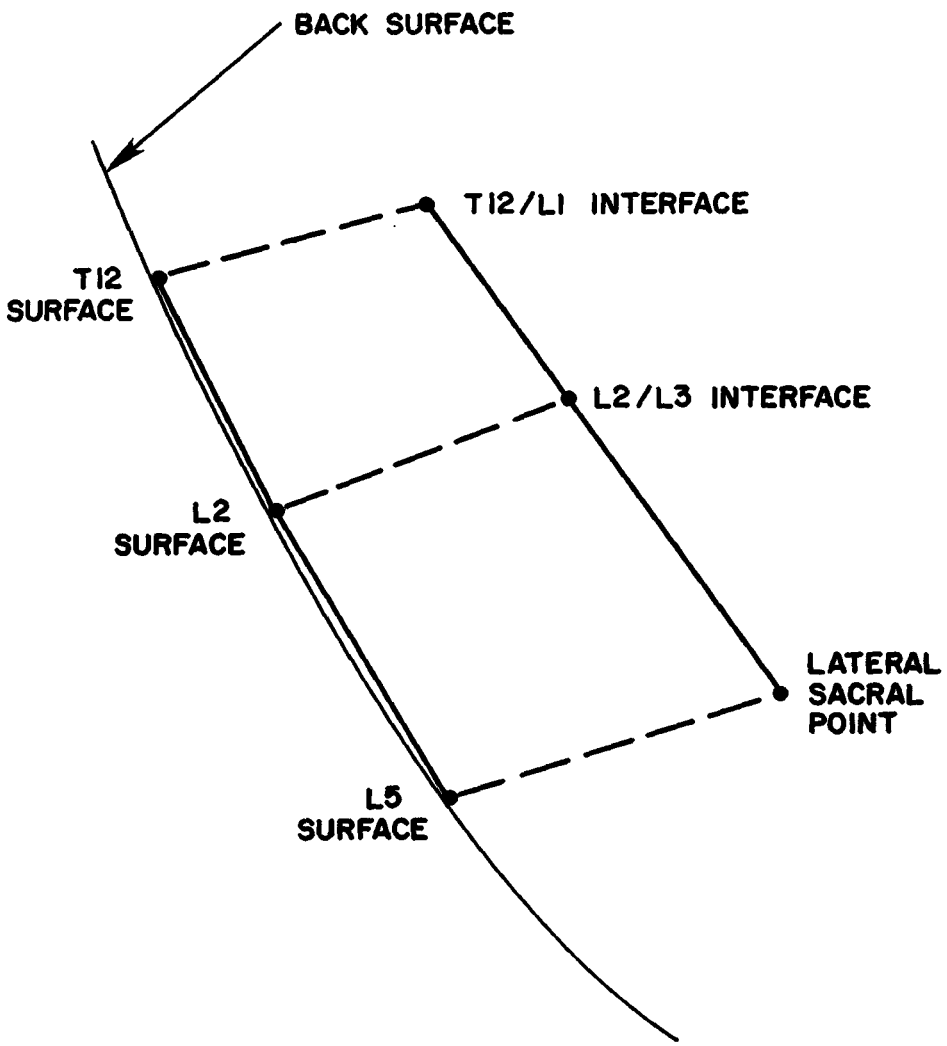

FIGURE 13. Construction of lumbar joints.

Figure 14 illustrates the location of the various elements in the shoulder girdle complex. Instead of a direct connection of the humerus to the thoracic skeleton, then, shoulder mobility should take into account this more complex linkage. Dempster (1965, 1955a, 1955b) has discussed this in detail and demonstrates differences in upper arm mobility when one or more of the joints are locked up. Figure 15 shows a superposition of three profiles of the maximum excursion curves traversed by the elbow if: (1) only the glenohumeral joint is free; (2) the glenohumeral and claviscapular joints are free; and (3) all three are free.

In the first case it should be noted that there does not appear to be much of a change in the center of rotation. Reuleaux analysis shows the center staying within the head of the humerus (Dempster 1955b); hence the center of the head of the humerus will now be called the glenohumeral joint. In the second case, it does not appear that there is much rotation or motion of the scapula with respect to the end of the clavicle. However, the rather small rotation of the free scapula allows large changes in the possible motions of the humerus. In the third case, the glenohumeral joint center (as well as the scapula and claviscapular joint) can undergo large motions with respect to the thorax as the clavicle rotates at its articulation with the sternum.

Dempster (1955a) has defined the sternoclavicular joint center as the "midpoint position of the palpable junction between the proximal end of the clavicle and the sternum at the upper border (jugular notch) of the sternum." It is estimated that this point is one centimeter below the clavicale surface landmark and 2 centimeters lateral from the body centerline. The laboratory coordinates of the sternoclavicular joint are thus:

$$X_H = -145,\ Y_H = \pm 20,\ Z_H = 433$$

The claviscapular joint center was defined as "the midpoint of a line between the coracoid tuberosity of the clavicle (at the posterior border of the bone) and the acromio-clavicular articulation (or the tubercle) at the lateral end of the clavicle; the point, however, should be visualized as on the underside of the clavicle." On the basis of

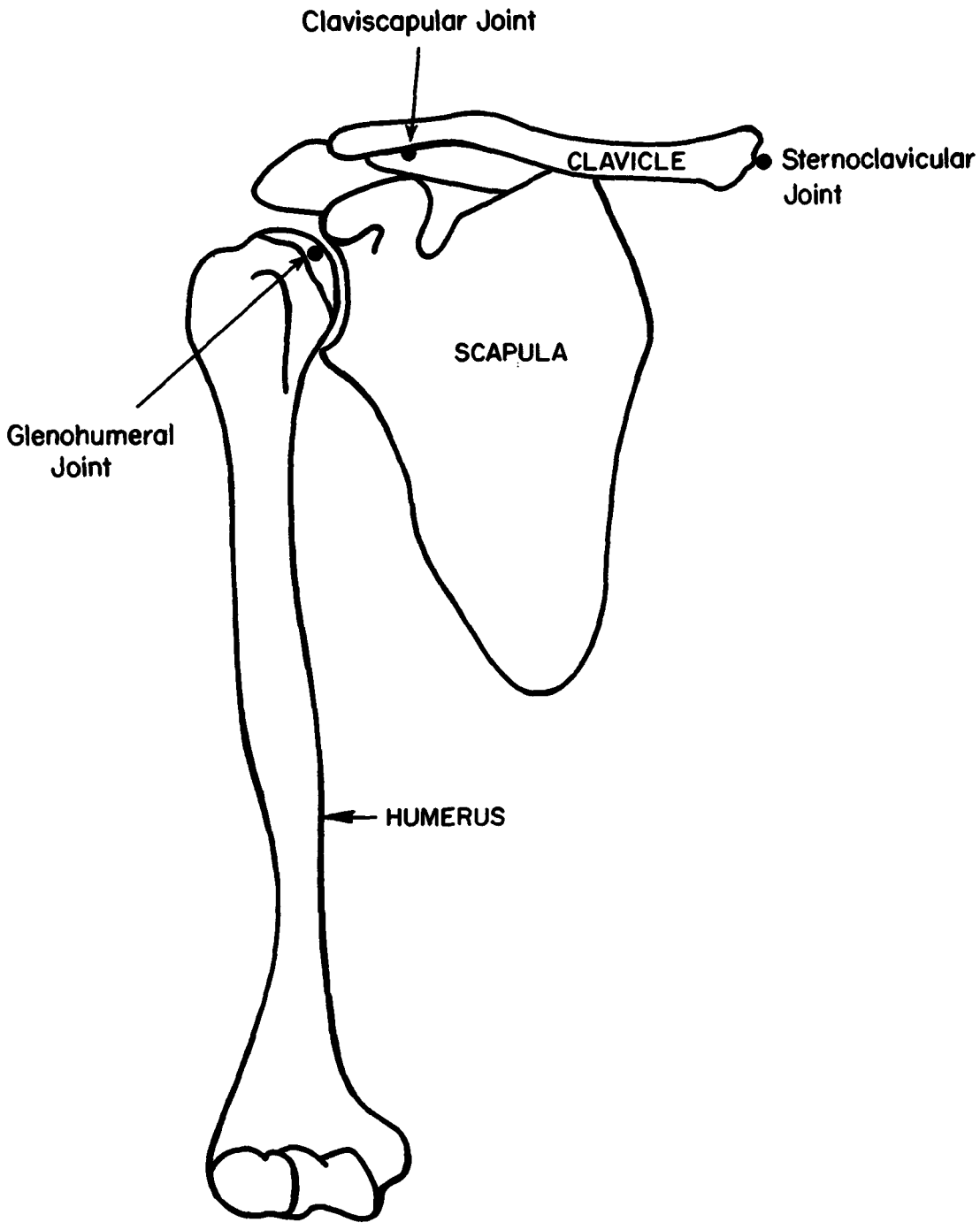

FIGURE 14. The three joints of the shoulder girdle.

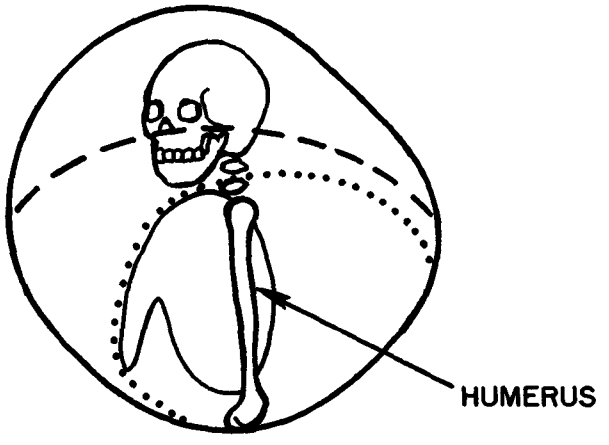

———— ALL THREE JOINTS FREE

– – – – – GLENOHUMERAL AND CLAVISCAPULAR JOINTS FREE

..... GLENOHUMERAL JOINT FREE

FIGURE 15. Range of motion at shoulder joint as a function of degrees of freedom.

measurements on skeletal material, it is estimated that the shift from the acromio-clavicular articulation surface landmark point is:

Y = 2.75/2 cm toward the center of the body
X = 1.5 cm toward the rear of the body
Z = 1 cm down

The estimated location of the claviscapular joint center is thus:

$$X_H=-230,\ Y_H=\pm 168,\ Z_H=427$$

The glenohumeral joint center is defined by Dempster (1955a) as the "midregion of the palpable bony mass of the head and tuberosities of the humerus, ..." The remainder of the definition prescribed an arm position in which to make a measurement which was not adaptable to presentation into precise three-dimensional coordinates. Three surface landmarks used during the present project define the location in space of the humerus with the assumption that the tissue depths are correct. These landmarks are:

Greater tubercle of the humerus
Lateral humeral epicondyle
Medial humeral epicondyle

A humerus with a 50th percentile length was set up in a three-dimensional measurement frame so that its coordinate system was parallel to the laboratory frame and so that the three skeletal landmarks were in locations prescribed in Table 4. The head of the humerus was modeled as a sphere so that the center could be determined from points on the surface. This construction yielded a glenohumeral joint center of:

$$X_H=-186,\ Y_H=\pm 173,\ Z_H=393$$

There was not sufficient time remaining in the project to complete a comparison of the shoulder girdle reconstruction based on these direct applications of Dempster with a reconstruction using the definitions and formula of the torso link study.

Dempster has defined the elbow joint to be the "midpoint of a line between (1) the lower palpable point of the medial epicondyle of the humerus, and (2) a point 8 mm above the radiale (radio-humeral

junction)." The two bony landmarks available from the present project which were used in this reconstruction were the radiale and the medial humeral epicondyle. The 8-mm point was chosen to be along an extension of the lower arm defined simply as a line from the ulnar styloid to the radiale. This resulted in a shift of the radiale point of X_H=-6, Z_H=-6 to form the point required under item (2). The elbow joint center was thus determined from the two points as:

$$X_H=36,\ Y_H=\pm 208,\ Z_H=201$$

The wrist joint has been added to the list of joints required in order to define a long axis of the forearm based on joint centers. Dempster's definition is that the joint is "on the palmar side of the hand, the distal wrist crease at the palmaris longus tendon, or the midpoint of a line between the radial styloid and the center of the pisiform bone; on the dorsal side of the hand, the palpable groove between the lunate and capitale bones, on a line with metacarpal bone III." It was estimated that for the UMTRI seated subjects the pisiform bone is approximately 20 mm distal in the X_H coordinate to the ulnar styloid, or can be approximated on the surface by the "pisiform surface location:"

$$X_H=246,\ Y_H=191,\ Z_H=387$$

An additional shift of Y_H=-10 is estimated to reach the pisiform bone centers which would be:

$$X_H=246,\ Y_H=181,\ Z_H=387$$

The wrist joint center can now be approximated by the center of a line connecting this point with the stylion as:

$$X_H=228,\ Y_H=158,\ Z_H=393$$

9.4 Joint Centers in Hip, Knee, and Ankle

The hip joint centers have been discussed in detail in Section 3. The center of the line connecting these points is used as the origin of the standard seat coordinate system. They have been developed based on symphysion and anterior-superior iliac spine surface landmarks in conjunction with the pelvic reconstruction of Reynolds et al. (1981).

Based on Dempster and Frankel et al. (1971) it is estimated that knee joint center can be approximated by the center of a line connecting the lateral and medial femoral epicondyles. The axis of the pin joint will be on a line perpendicular to the plane formed by the lines connecting joint centers in the upper and lower legs. The center of the line, which is based on two available surface landmarks, is:

$$X_H=406,\ Y_H=\pm 138,\ Z_H=136$$

The ankle joint center has been defined by Dempster to be on the "level of a line between the tip of the lateral malleolus of the fibula and a point 5 mm distal to the tibial malleolus. The distal translation is further down the leg from the sphyrion which involves both X_H and Z_H translations for the seated occupant of $X_H=3$, $Z_H=-4$. So the ankle joint center is at the center of the line connecting the shifted sphyrion landmark with the lateral malleolus of the fibula which was also measured in the current project. Its coordinates are:

$$X_H=684,\ Y_H=94,\ Z_H=-169$$

10.0 JOINT PARAMETERS

10.1 Introduction

There are two basic types of parameters which should be considered in the development of joint parameters. The first of these is an identification of the normal range of mobility between different segments of the body. The second is the resistance to motion when one segment of the body moves with respect to its neighbors.

The normal range of mobility of the body is usually described as joint range of motion data. The most commonly used sources are Dempster (1955a), Barter et al. (1957), and Glanville and Kreezer (1937). References with particularly extensive data on neck mobility have been prepared by Ferlic (1962) and Snyder et al. (1975a, 1975b). Thoracic and lumbar spine mobility data have been reported by Nyquist and Murton (1975) as well as Mital et al. (1978, 1979) and Krieger (1976). The Mital work at Wayne State University is part of activity under Department of Transportation Contract No. DOT-HS-5-01232. The thoracic and lumbar range of motion data in the coronal plane and about the vertebral axes, which have been gathered under that contract, are in draft report form. Additional extensive range-of-motion data on head/neck flexion, extension, lateral flexion, rotation, and combined modes are expected in the near future from the Naval Aeromedical Research Laboratory in New Orleans.

Data on resistance to motion is very much more difficult to find, interpret, and assemble into a form usable in dummy design work. The most directly applicable data have been reported for the:

- Neck by Mertz and Patrick (1971), Snyder et al. (1975a, 1975b), and Robbins et al. (1974)
- Head/trunk, waist, hip, knee, shoulder, elbow by Krieger (1976)
- Lower spine by Nyquist and Murton (1975) and Mital et al. (1978, 1979)
- Shoulder, arms, and legs by Engin (1979, 1980, 1981), Engin and Kaleps (1980), and Engin and Kazarian (1981)

The final two subsections of the report cover the two basic issues just sketched out--range of motion at joint structures and resistance to motion at joint structures.

10.2 Range of Motion at Joint Structures

Dempster (1955a) has gathered the most comprehensive set of range of voluntary motion data. These were reanalyzed, graphically illustrated, and reported in an easier to understand format by Barter et al. (1957). Dempster did not report range-of-motion data for the spinal column or abductions in the coronal plane for the shoulder. Traditional data on the neck and shoulder are available from Glanville and Kreezer (1937) while more recent data of Snyder et al. (1975a, 1975b) supplement the neck information. Available thoracic and lumbar spine mobility are limited to flexion studies by Nyquist and Murton (1975) and Mital et al. (1978, 1979).

Table 21 is a summary of range-of-motion data with the source indicated. The various measures are illustrated in Figure 16. The coronal plane corresponds to a $Y_H Z_H$ plane for a standing person while the transverse plane is an $X_H Y_H$ plane. The sagittal plane ($X_H Z_H$) is the plane of flexion and extension.

10.3 Resistance to Motion at Joint Structures

For the neck, the corridor proposed by Mertz and Patrick (1971) is the best available description of neck resistance to motion in flexion and extension. These data, illustrated in Figure 17, are already in use in dummy construction and give values of torque at the occipital condyles versus head rotation angle relative to the torso.

In the case of lateral flexion, the only known data are derived from the lateral hyperflexion injury study at UMTRI (Snyder et al. 1975b). Using head jerk test data, a computer simulation was used to estimate spring rates of about 16 in. lb/degree of lateral flexion for small motions. Figure 18 shows a hypothesized form for resistance to lateral flexion. The dotted line represents stiffening at the end of the voluntary motion range.

No data are known to be available for neck rotation. However, some are anticipated based on analyses currently being conducted on NAMRL data.

All data known to the present author for the vertebral column have been gathered by Nyquist and Murton (1975), Mital et al. (1978, 1979), and Krieger (1976). The slope of the Krieger data appear to fall within the bounds set by Nyquist and Murton. A simple version of the Krieger data, with increased stiffness at the end of the range of motion is shown in Figure 19. Lateral flexion and rotation about the axis of the spinal column are not yet available but should appear in the near future under DOT contract No. DOT-HS-5-01232.

Engin (1980) provides a considerable body of information on the overall resistance of the shoulder complex to rotation. Not only are extension and flexion in the sagittal plane given but also the rotation about the long axis of the humerus. Figure 20 illustrates part of Engin's information. The data shown give only the maximum moment curve at the joint. Engin has developed the complete three-dimensional moment vector. Further information on the force resistance to shrugging motions is also presented (Engin 1981).

Krieger has provided some limited information on the elbow. Figure 21 is a simple model for the untensed elbow with a stiffness at the fully flexed position less than that for the extended position. Engin (1979) and Engin and Kaleps (1980) also provided torque/angle information on pronation and supination of the hand at the wrist.

Hip flexion and extension data have been developed by both Nyquist and Murton (1975) and Krieger (1976). As is the case with the spinal data, Nyquist and Murton report very different results for the cases of relaxed or tensed subjects. Further they suggest that: "A decision should be made with regard to dummy design philosophy. Should the dummy respond as a relaxed or as a tensed human, or perhaps in accordance with some intermediate criteria?" An idealized version of Krieger's data is shown in Figure 22. Data on resistance to rotation about the long axis of both the femur and tibia are available based on the work of Engin (1979) and Engin and Kaleps (1980).

Data on torque at the knee are available from a variety of sources including Krieger (1976) and Robbins et al. (1971). An idealization of Krieger's data is included as Figure 23. A part of a study of human volunteer sled test subjects involved a measurement of the amount of knee tensing which is possible. A maximum value of 5040 in.lb. was measured which is the equivalent of 20 Gs of joint strength. This emphasizes the comment of Nyquist and Murton made in the previous paragraph.

In summary, a variety of data are available which raises some hope that it may be possible to make estimates for joint ranges of motion and resistance to such motions. Questions must be answered as to whether to define a range of performance based on free-moving or tensed joints. Some data gaps must be filled and the results of the various investigators pulled together in a consistent format.

TABLE 21

RANGE-OF-MOTION DATA

Quantity	Value (deg)	Reference
Head		
Ventral flexion	55 (60)	
Dorsal flexion (hyperextension)	49 (61)	Snyder et al. (1975a,b)
Lateral Flexion	35 (41)	(Glanville & Kreezer 1937)
Rotation	67 (74)	
Vertebral Column		
Rotation of T1 with respect to T12 (flexion)	15	Mital et al. (1979)
Rotation of T12 with respect to pelvis (flexion)	16	Mital et al. (1979)
Rotation of T1 with respect to T12 (extension)	20	Mital et al. (1979)
Rotation of T12 with respect to pelvis (extension)	7	Mital et al. (1979)
Lateral flexion	42 ?	Robbins et al. (1971)
Rotation about long axis	±45 ?	(Con. No. DOT-HS-5-01232)
Shoulder (Three Links)		
Flexion (sagittal plane)	188	Dempster (1955a)
Extension (sagittal plane)	61	Dempster (1955a)
Abduction (coronal plane)	129	Glanville & Kreezer (1937)
Abduction (transverse plane)	134	Dempster (1955a)
Adduction (transverse plane)	48	Dempster (1955a)
Shoulder (Clavicle Link)		
Protraction (transverse plane)	15	(Derived from
Retraction (transverse plane)	20	Dempster 1955a)
Depressed (coronal plane)	8	
Shrugged (coronal plane)	36	
Elbow		
Extension	0	Dempster (1955a)
Flexion	142	Dempster (1955a)
Hip		
Flexion	113 (168)	Dempster (1955a) (Glanville & Kreezer 1937)
Abduction (transverse plane)	53	Dempster (1955a)
Adduction (transverse plane)	31	Dempster (1955a)
Abduction (coronal plane)	70	Glanville & Kreezer (1937)
Medial rotation (prone)	39	Dempster (1955a)
Lateral rotation (prone)	34	Dempster (1955a)
Medial rotation (sitting)	31	Dempster (1955a)
Lateral rotation (sitting)	30	Dempster (1955a)

TABLE 21
RANGE OF MOTION DATA (Continued)

Quantity	Value (deg)	Reference
Knee		
Voluntary flexion (prone)	125	Dempster (1955a)
Forced flexion	144	Dempster (1955a)
Forced flexion (kneeling)	159	Dempster (1955a)
Medial rotation	35	Dempster (1955a)
Lateral rotation	43	Dempster (1955a)
Ankle		
Dorsiflexion	35	Dempster (1955a)
Plantar flexion	38	Dempster (1955a)
Inversion	24	Dempster (1955a)
Eversion	23	Dempster (1955a)

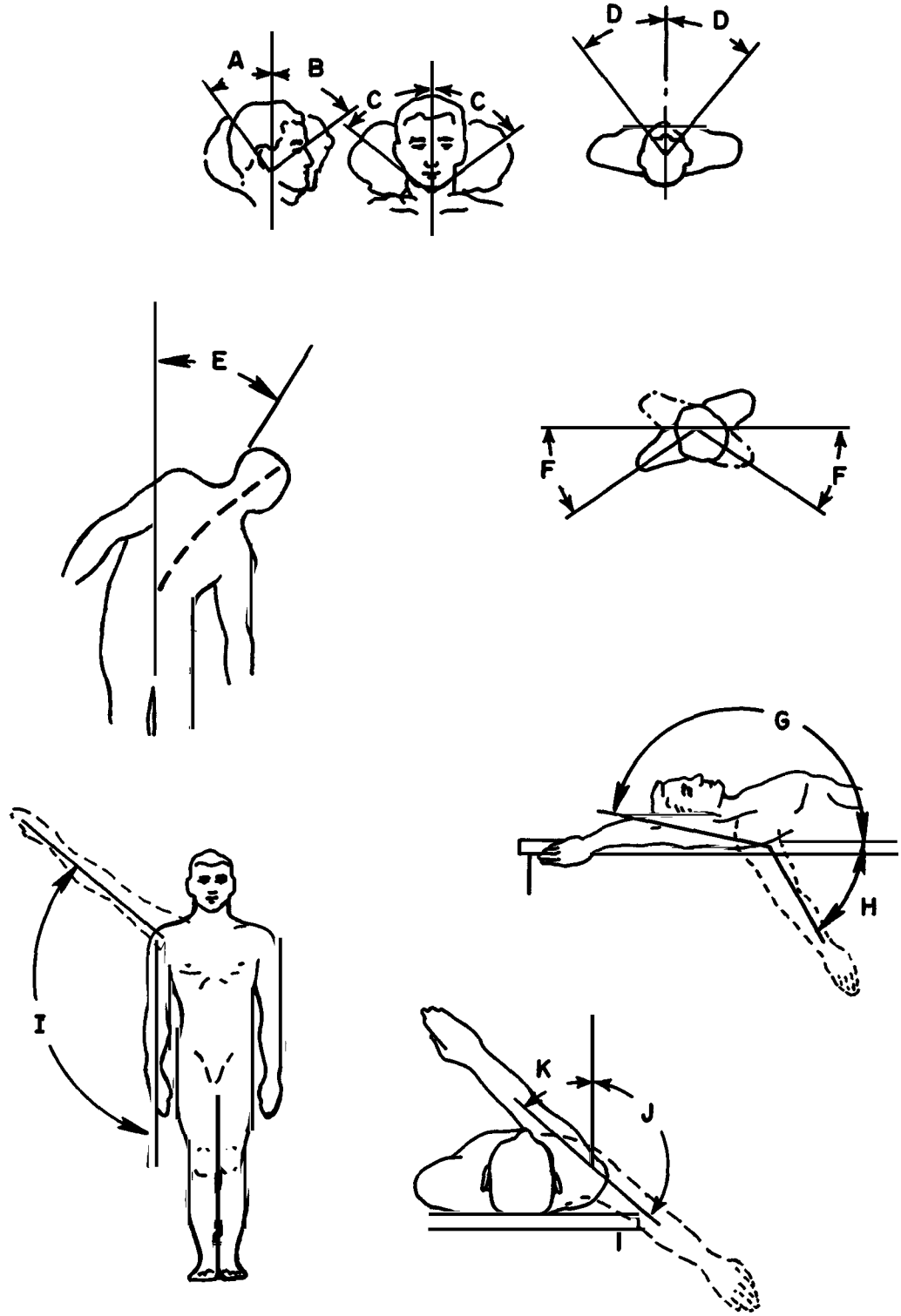

FIGURE 16. Illustrations of range-of-motion definitions (1 of 4).

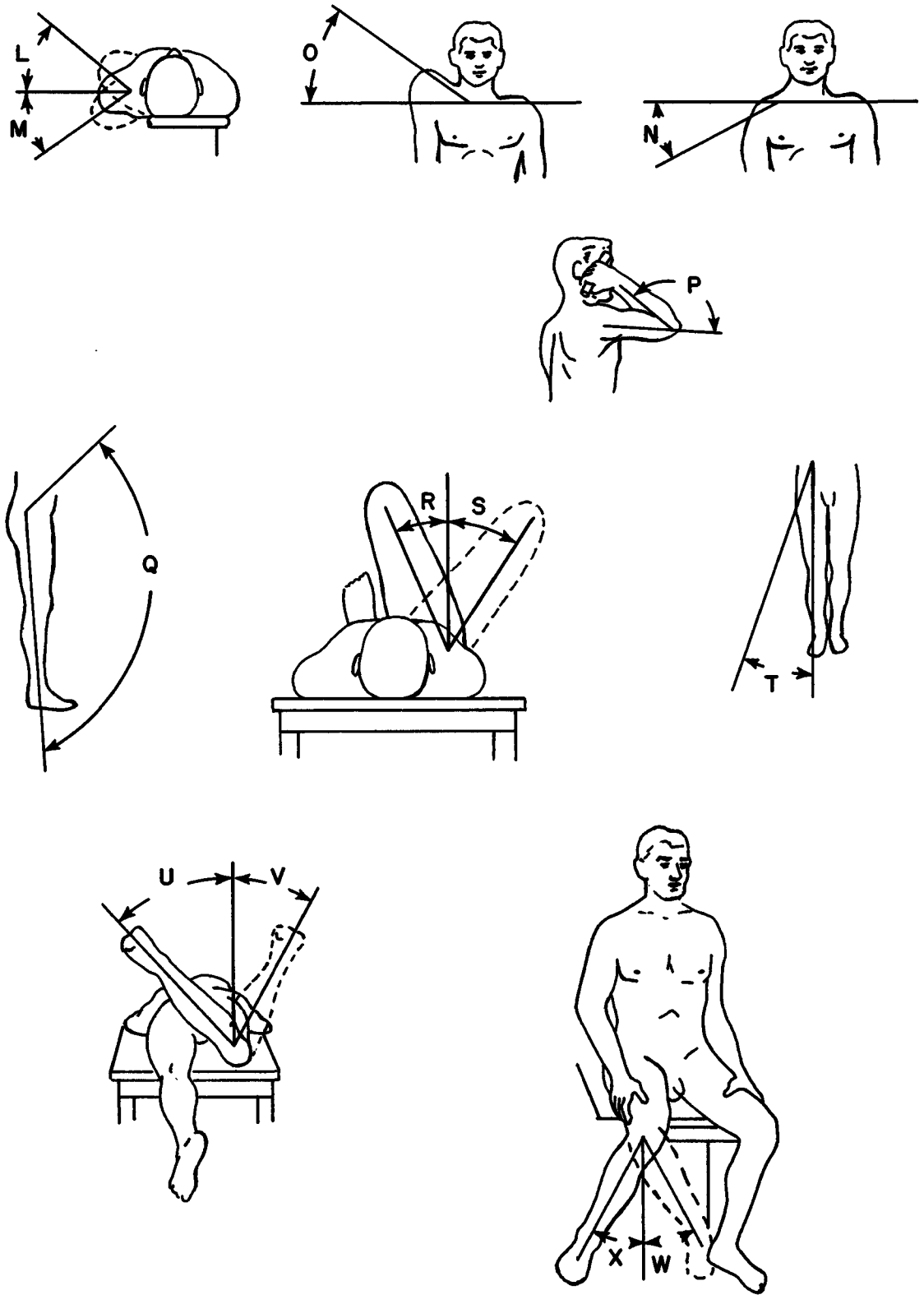

FIGURE 16. Illustrations of range-of-motion definitions (2 of 4).

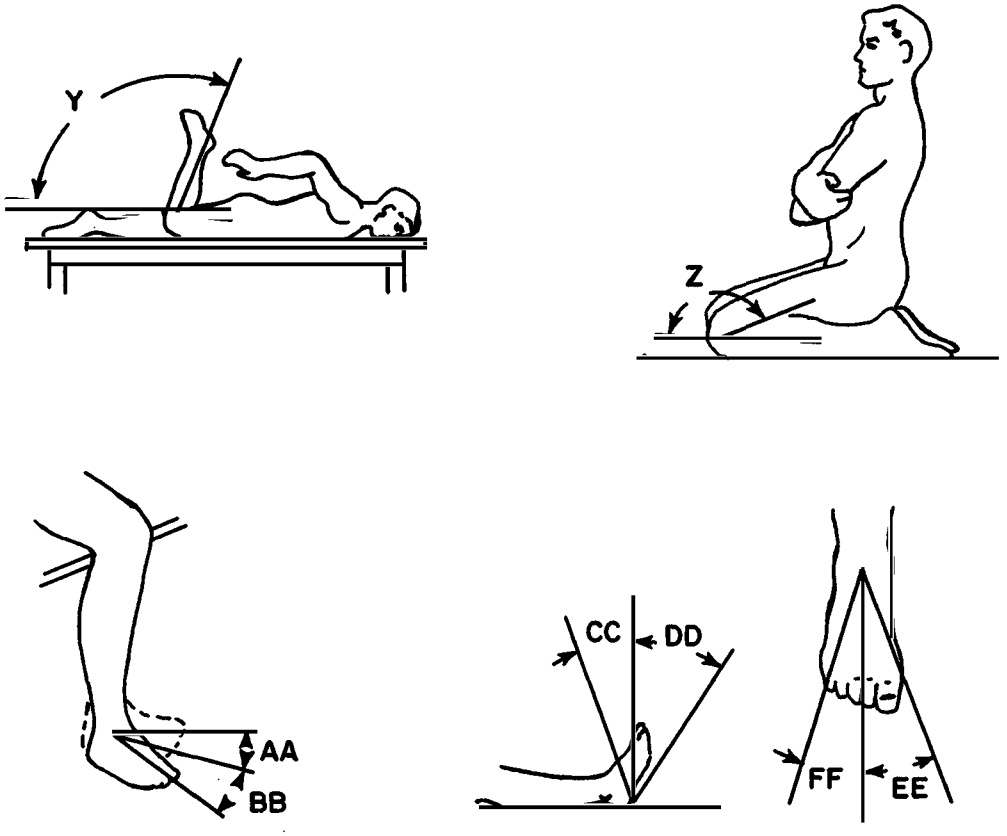

FIGURE 16. Illustrations of range of motion definitions (3 of 4).

Range-of-Motion Illustration Code

A - Head dorsal flexion (hyperextension)
B - Head ventral flexion
C - Head lateral flexion
D - Head rotation
E - Torso lateral flexion
F - Torso rotation about long axis
G - Shoulder flexion (sagittal plane) (3 links)
H - Shoulder extension (sagittal plane) (3 links)
I - Shoulder abduction (coronal plane) (3 links)
J - Shoulder abduction (transverse plane) (3 links)
K - Shoulder adduction (transverse plane) (3 links)
L - Shoulder protraction (transverse plane) (clavicle)
M - Shoulder retraction (transverse plane) (clavicle)
N - Shoulder depressed (coronal plane) (clavicle)
O - Shoulder shrugged (coronal plane) (clavicle)
P - Elbow flexion
Q - Hip flexion
R - Hip abduction (transverse plane)
S - Hip adduction (transverse plane)
T - Hip abduction (coronal plane)
U - Hip medial rotation (prone)
V - Hip lateral rotation (prone)
W - Hip medial rotation (sitting)
X - Hip lateral rotation (sitting)
Y - Knee voluntary flexion (prone)
Z - Knee forced flexion (kneeling)
AA - Knee medial rotation
BB - Knee lateral rotation
CC - Ankle dorsiflexion
DD - Ankle plantar flexion
EE - Ankle inversion
FF - Ankle eversion

FIGURE 16. Illustrations of range-of-motion definitions (4 of 4).

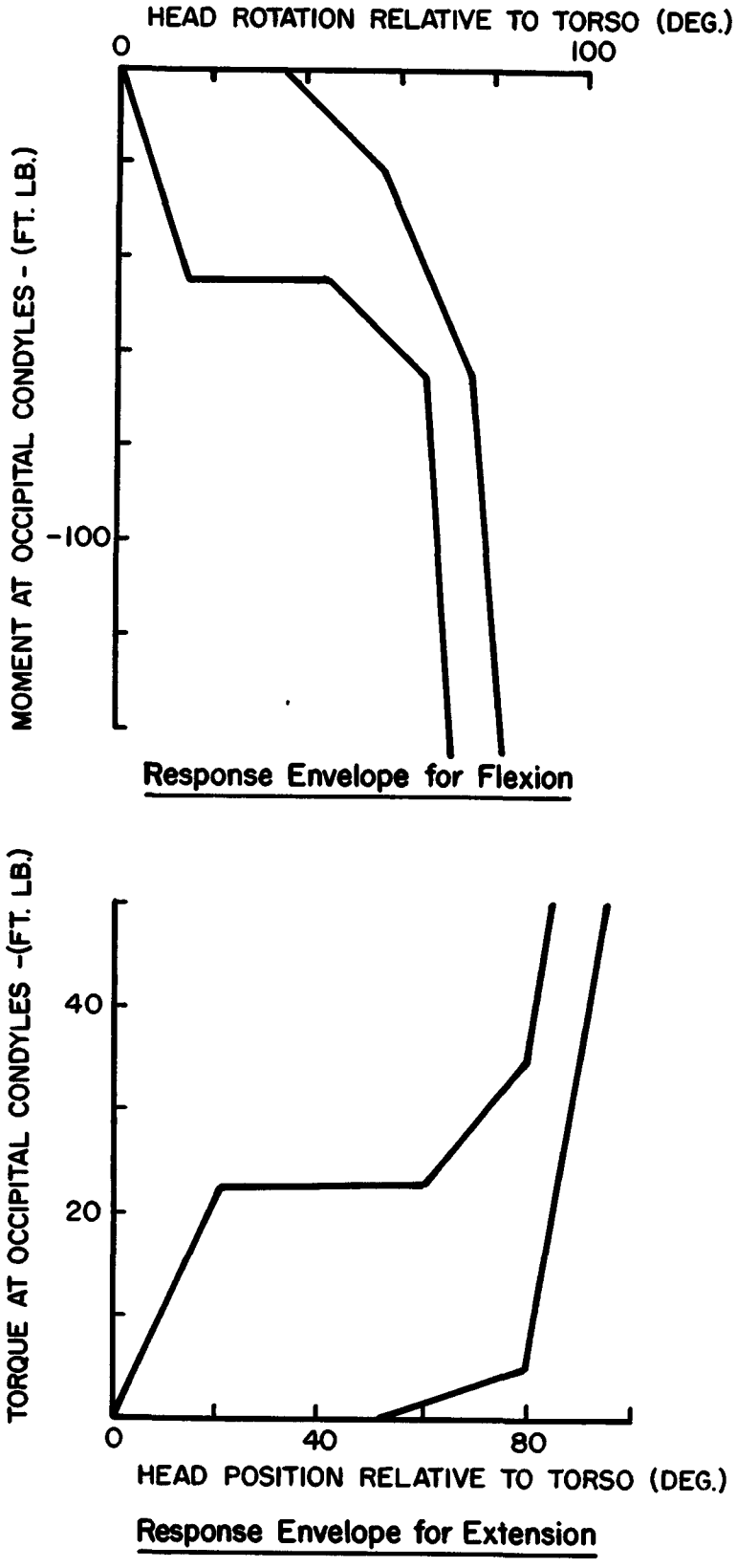

FIGURE 17. Head resistance to flexion and extension (after Mertz and Patrick 1971).

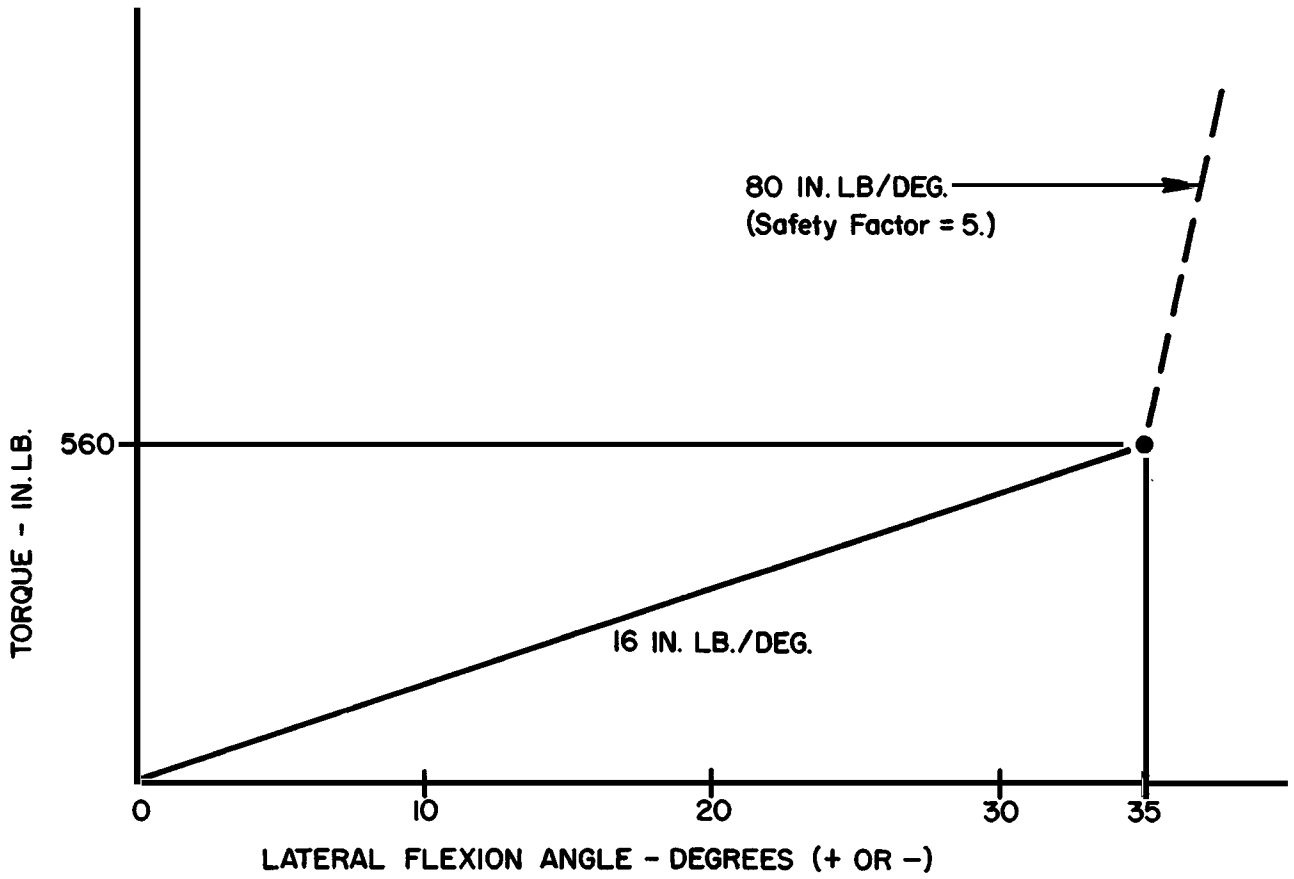

FIGURE 18. Head resistance to lateral flexion (after Snyder et al. 1975b).

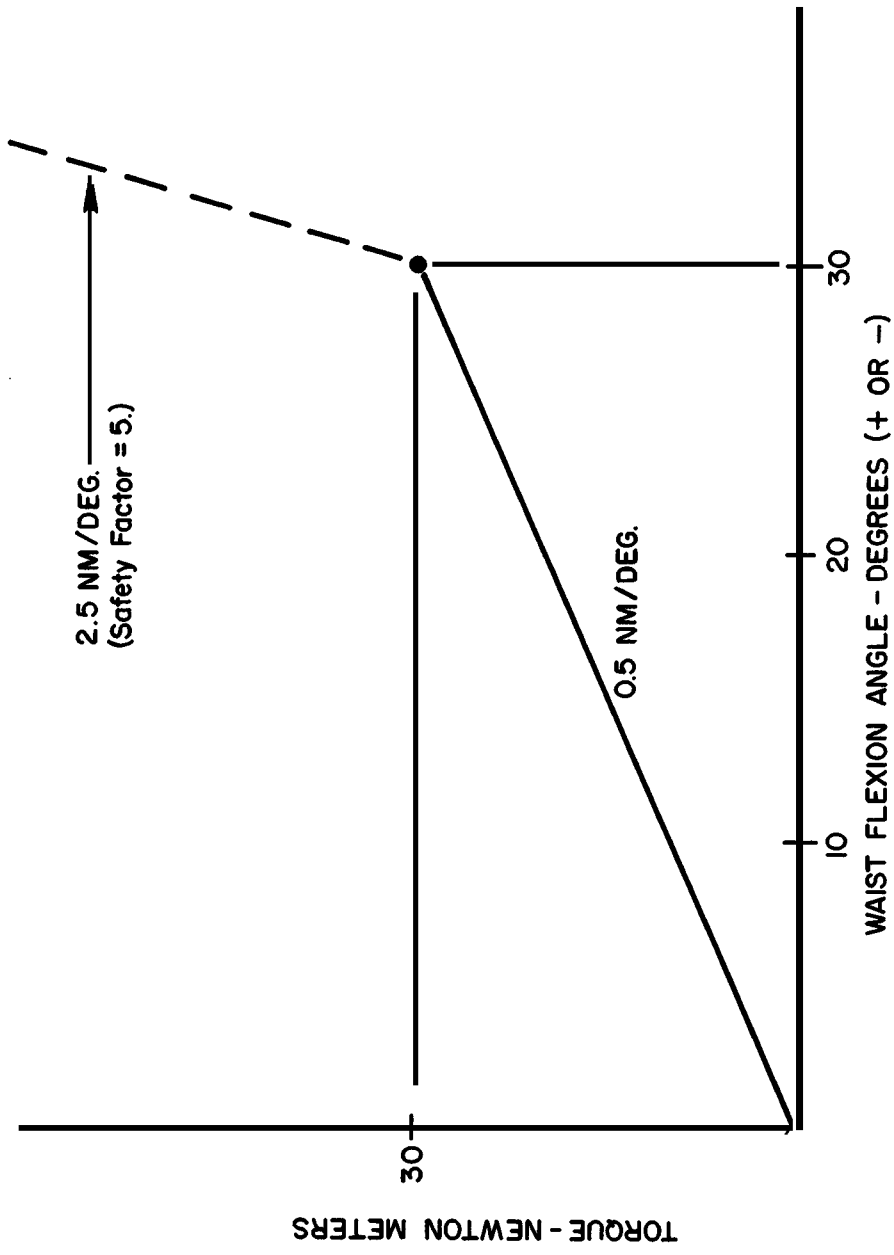

FIGURE 19. Waist resistance to flexion and extension (after Krieger 1976).

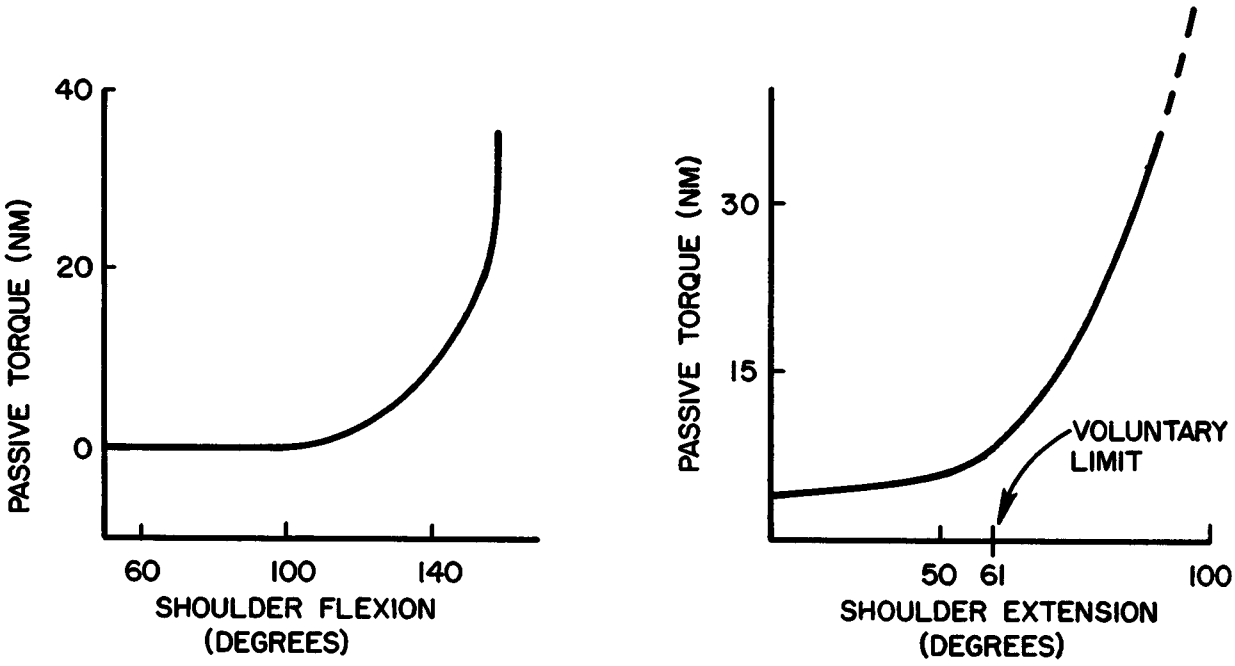

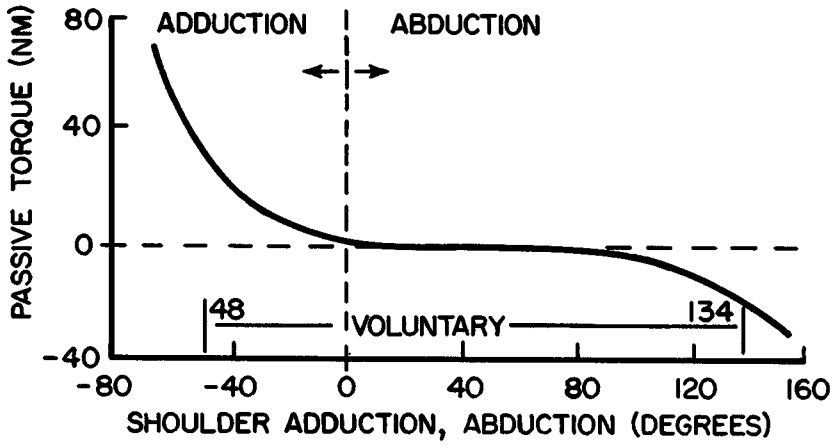

FIGURE 20. Shoulder resistance to rotation (after Engin 1980).

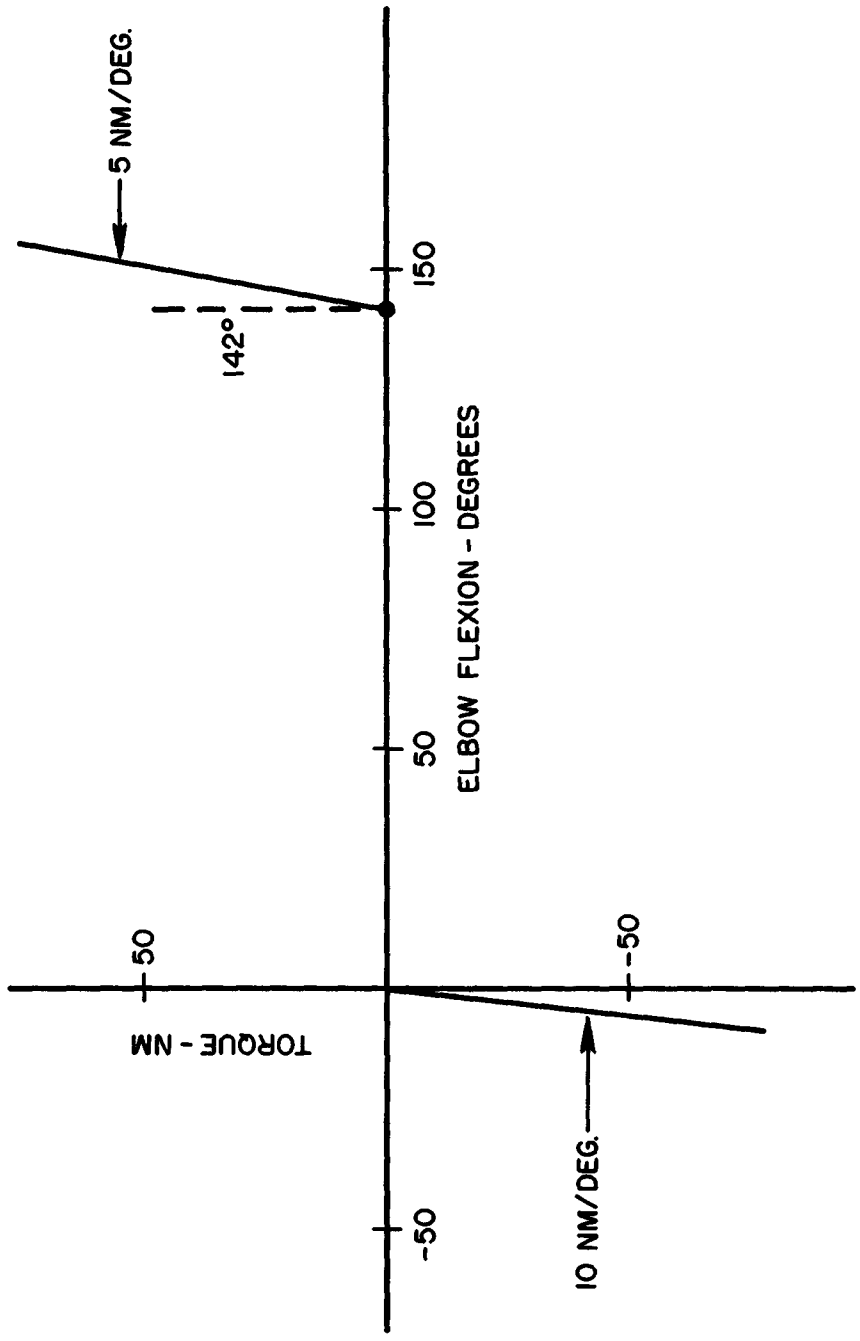

FIGURE 21. Elbow resistance to flexion (after Krieger 1976).

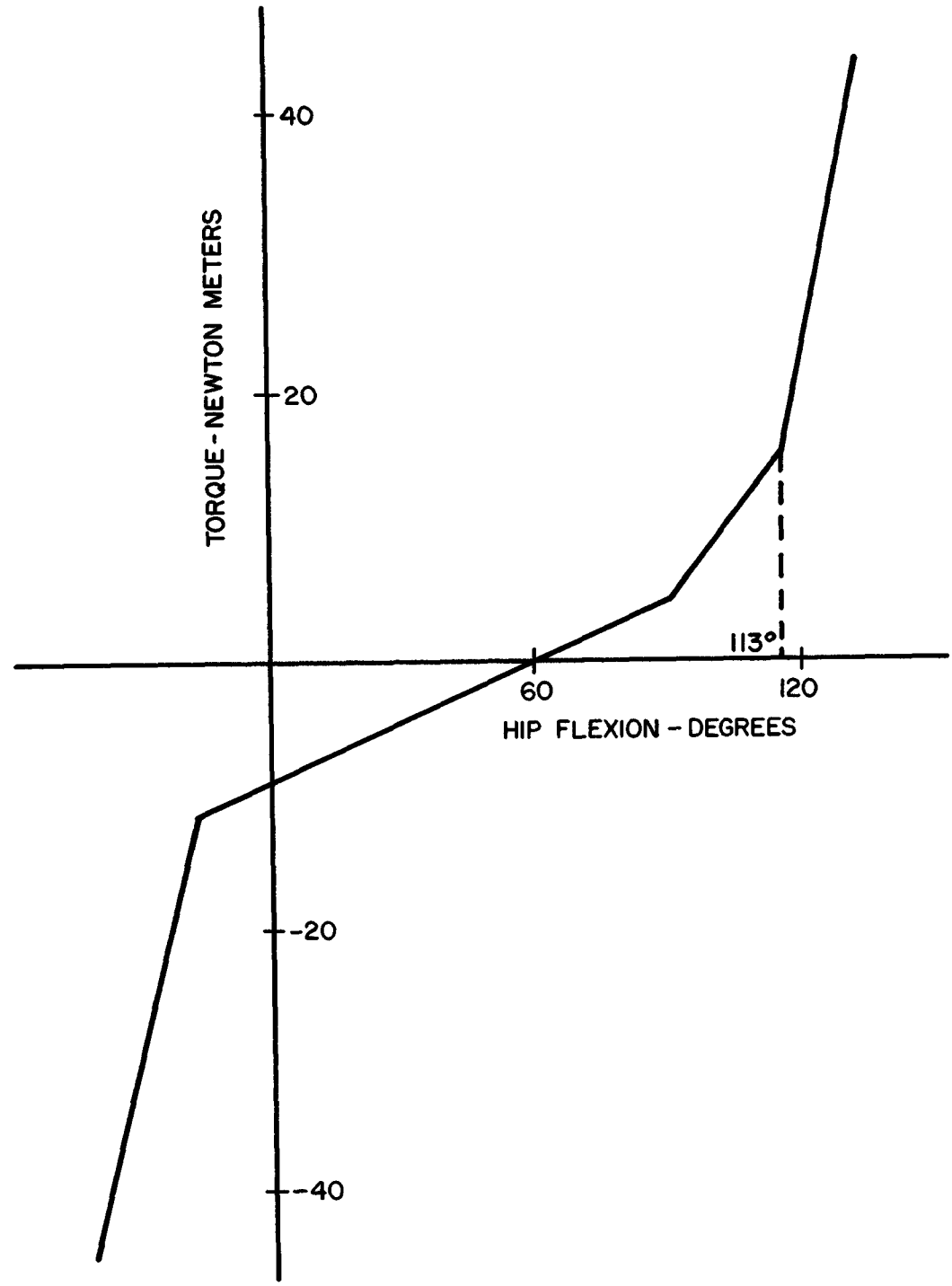

FIGURE 22. Resistance to hip flexion and extension (after Krieger 1976).

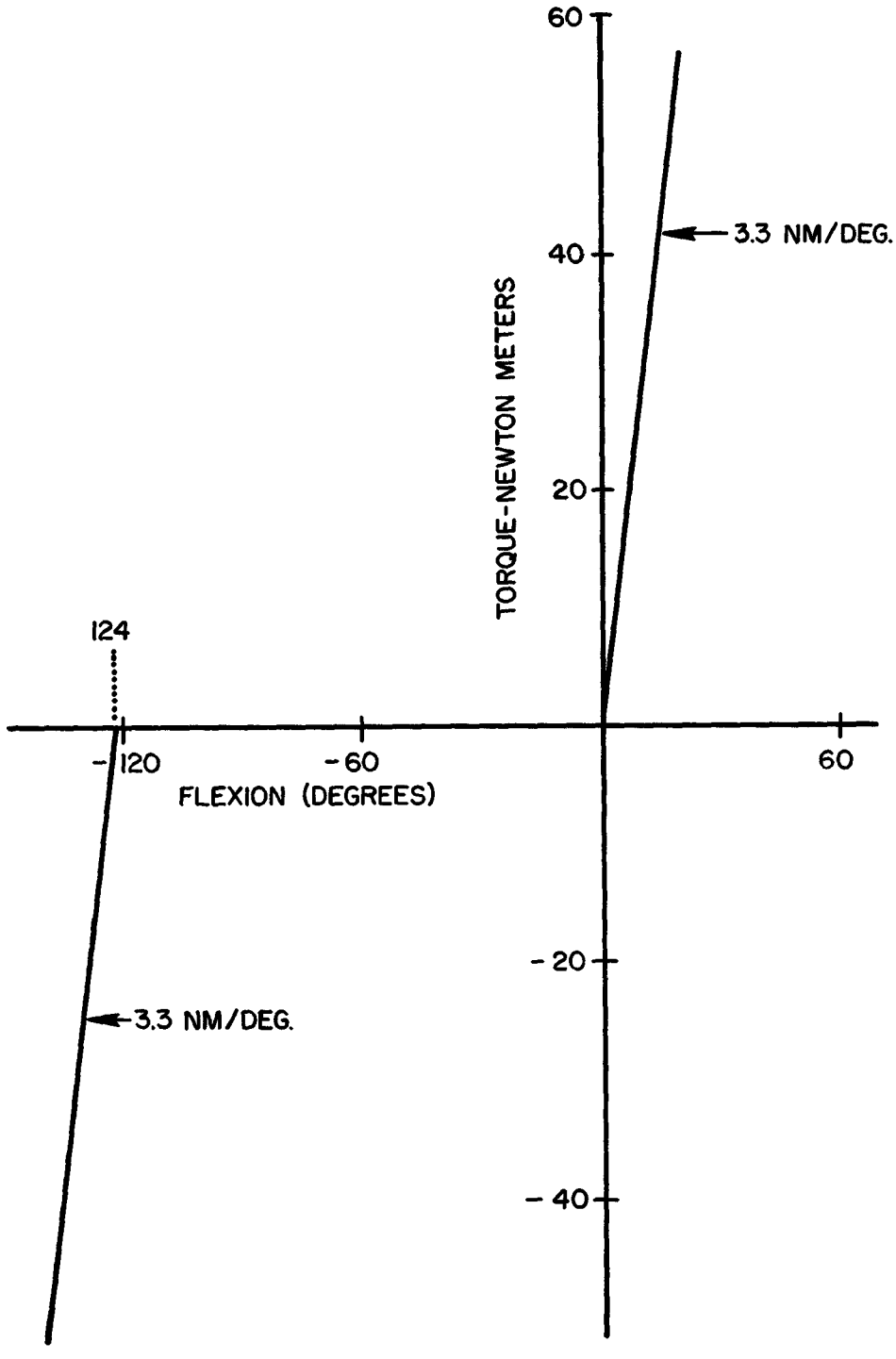

FIGURE 23. Resistance to flexion at knees (after Krieger 1976).

11.0 REFERENCES

Barter, J.T.; Emanuel, I.; and Truett, B. (1957) A statistical evaluation of joint range data. Wright-Patterson AFB, Wright Air Development Center, WADC TN-57-311.

Beier, G.; Schuller, E.; Schuck, M.; Ewing, C.L.; Becker, E.D.; and Thomas, D.J. (1980) Center of gravity and moments of inertia of human heads. Proc. 5th International IRCOBI Conference on the Biomechanics of Impacts, pp. 218-228. Edited by J.P. Cotte and A. Charpenne. IRCOBI, Bron.

Bowman, B.M.; and Robbins, D.H. (1972) Parameter study of biomechanical quantities in analytical neck models. Proc. 16th Stapp Car Crash Conference, pp. 14-44.

Bowman, B.M.; Bennett, R.O.; and Robbins, D.H. (1979) MVMA two-dimensional crash victim simulation, Version 4. The University of Michigan, Highway Safety Research Institute, Report No. UM-HSRI-79-5-1.

Chandler, R.F.; and Young, J. (1981) Uniform mass distribution properties and body size appropriate for the 50th percentile male aircrewmember during 1980-1990. Federal Aviation Administration, Memorandum Report No. AAC-119-81-4.

Cheng, R.; Mital, N.K.; Levine, R.S.; and King, A.I. (1979) Biodynamics of the living spine during -Gx impact acceleration. Proc. 23rd Stapp Car Crash Conference, pp. 721-764.

Churchill, E.; and Truett, B. (1957) Metrical relations among dimensions of the head and face. Wright-Patterson AFB, Wright Air Development Center, WADC-TD-56-621.

Clauser, C.E.; McConville, J.T.; and Young, J.W. (1969) Weight, volume, and center of mass of segments of the human body. Wright-Patterson AFB, Aerospace Medical Research Laboratory, AMRL-TR-69-70.

Dempster, W.T. (1955a) Space requirements of the seated operator. Wright-Patterson AFB, Wright Air Development Center, WADC-TR-55-159.

Dempster, W.T. (1955b) The anthropometry of body action. New York Academy of Sciences Annals, 63:559-585.

Dempster, W.T. (1965) Mechanics of shoulder movement. Archives of Physical Medicine and Rehabilitation, 46:49-69.

Dempster, W.T.; and Gaughran, G.R.L. (1967) Properties of body segments based on size and weight. American Journal of Anatomy, 120:33-54.

Engin, A.E. (1979) Passive resistive torques about long bone axes of major human joints. Aviation, Space, and Environmental Medicine, 50:1052-57.

Engin, A.E. (1980) On the biomechanics of the shoulder complex. Journal of Biomechanics, 13:575-590.

Engin, A.E. (1981) Long bone and joint response to mechanical loading. Ohio State University for Air Force Office of Scientific Research. Bolling Air Force Base, Contract F49620-79-C-0110.

Engin, A.E.; and Kaleps, I. (1980) Active muscle torques about long-bone axes of major human joints. Aviation, Space, and Environmental Medicine, 51:551-555.

Engin, A.E.; and Kazarian, L. (1981) Active muscle force and moment response of the human arm and shoulder. Aviation, Space, and Environmental Medicine, 52:523-530.

Ewing, C.L.; and Thomas, D.J. (1972) Human head and neck response to impact acceleration. Naval Aerospace medical Research Laboratory, Monograph 21.

Ewing, C.L.; and Thomas, D.J. (1973) Response of human head to impact. Proc. 17th Stapp Car Crash Conference, pp. 309-342.

Ferlic, D. (1962) The range of motion of the normal cervical spine. Hopkins Hospital Bulletin, 110.

Foster, J.K.; Kortge, J.O.; and Wolanin, M.J. (1977) Hybrid III--A biomechanically based crash test dummy. Proc. 21st Stapp Car Crash Conference, pp. 973-1014.

Frankel, V.H.; Burstein, A.H.; and Brooks, D.B. (1971) Biomechanics of internal derangement of the knee. Journal of Bone and Joint Surgery, 53A:945-962.

Glanville, A.D.; and Kreezer, G. (1937) The maximum amplitude and velocity of joint movements in normal male human adults. Human Biology, 9:197-211.

Kaleps, I. (1982) Phone conversations, July 20 and 27.

Krieger, K. (1976) Full scale experimental simulation of pedestrian-vehicle impacts. Ph.D. dissertation, Wayne State University, Detroit.

McConville, J.T.; Churchill, T.D.; Kaleps, I.; Clauser, C.E.; and Cuzzi, J. (1980) Anthropometric relationships of body and body segment moments of inertia. Wright-Patterson AFB, Aerospace Medical Research Laboratory, AMRL-TR-80-119.

Mertz, H.J.; and Patrick, L.M. (1971) Strength and response of the human neck. Proc. 15th Stapp Car Crash Conference, pp. 207-255.

Mital, N.K.; Cheng, R.; Levine, R.S.; and King, A.I. (1978) Dynamic characteristics of the human spine during -Gx acceleration. Proc. 22nd Stapp Car Crash Conference, pp. 139-165.

Mital, N.K.; Cheng, R.; King, A.I.; and Eppinger, R.H. (1979) A new design for a surrogate spine. Proc. 7th International Technical Conference on Experimental Safety Vehicles, pp. 427-428. U.S. Government Printing Office, Washington, D.C.

Nyquist, G.W.; and Murton, C.J. (1975) Static bending response of the lower human torso. Proc. 19th Stapp Car Crash Conference, pp. 513-541.

Reynolds, H.M.; Clauser, C.E.; McConville, J.; Chandler, R.; and Young, J.W. (1975) Mass distribution properties of the male cadaver. SAE paper no. 750424.

Reynolds, H.M.; Snow, C.C.; and Young, J.W. (1981) Spatial geometry of the human pelvis. Federal Aviation Administration, Memorandum Report No. AAC-119-81-5.

Robbins, D.H. (1977) Errors in definition of an anatomically based coordinate system using anthropometric data. In Task Report, Phase I, Interim Report to AFOSR, Contract F44620-76-C-0115, Highway Safety Research Institute, The University of Michigan.

Robbins, D.H.; Snyder, R.G.; and Roberts, V.L. (1971) Mathematical simulation of daisy track human volunteer tests. The University of Michigan, Highway Safety Research Institute, HSRI-BIOM-71-6.

Robbins, D.H.; Snyder, R.G.; Chaffin, D.B.; and Foust, D.R. (1974) A mathematical study of the effect of neck physical parameters on injury susceptibility. SAE paper no. 740274.

Schneider, L.W.; Foust, D.R.; Bowman, B.M.; Snyder, R.G.; Chaffin, D.B.; Abdelnour, T.R.; and Baum, J.K. (1975) Biomechanical properties of the human neck in lateral flexion. Proc. 19th Stapp Car Crash Conference, pp. 455-485.

Snyder, R.G.; Chaffin, D.B.; and Schutz, R.K. (1972) Link system of the human torso. Wright-Patterson AFB, Aerospace Medical Research Laboratory, AMRL-TR-71-88.

Snyder, R.G.; Chaffin, D.B.; and Foust, D.R. (1975a) Bioengineering study of basic physical measurements related to susceptibility to cervical hyperextension-hyperflexion injury. The University of Michigan, Highway Safety Research Institute, UM-HSRI-BI-75-6.

Snyder, R.G.; Chaffin, D.B.; Schneider, L.W.; Foust, D.R.; Bowman, B.M.; Abdelnour, T.A.; and Baum, J.K. (1975b) Basic biomechanical properties of the human neck related to lateral hyperflexion injury. The University of Michigan, Highway Safety Research Institute, UM-HSRI-BI-75-4.